RSC Advances

REVIEW

View Article Online
View Journal | View Issue

Cite this: *RSC Adv.*, 2025, **15**, 29627

Recent advances in the antimicrobial application of the pyrrolo[2,3-*d*]pyrimidine scaffold: innovative synthetic strategies, structural diversification, and bioactivity evaluation

Zhaoju Sun,†[a] Ting Li,†[a] Yi He,†[b] Hongwu Liu,[a] Linli Yang,[a] Zhibing Wu,[a] Liwei Liu,[a] Zhenbao Luo,*[b] Xiang Zhou *[a] and Song Yang *[a]

Antimicrobial resistance (AMR) has emerged as a critical global health challenge, necessitating urgent development of novel antimicrobial agents. Pyrrolo[2,3-*d*]pyrimidine derivatives have garnered substantial research interest in pharmaceutical chemistry owing to their structural diversity, synthetic accessibility, and broad-spectrum bioactivity. This comprehensive review presents and discusses recent advancements in pyrrolo[2,3-*d*]pyrimidine research, focusing on methodological innovations in scaffold construction. Key synthetic strategies, including [3 + 2] cycloadditions, transition metal-catalyzed couplings, and microwave-assisted ring closure techniques, are highlighted. Additionally, a thorough discussion of their antimicrobial activities is presented, encompassing antibacterial, antifungal, and antiviral effects. This review provides valuable insights into the rational design and synthesis of novel pyrrolo[2,3-*d*]pyrimidine derivatives. These contributions may facilitate the development of new antimicrobial agents to address evolving resistance.

Received 11th May 2025
Accepted 15th July 2025

DOI: 10.1039/d5ra03313f

rsc.li/rsc-advances

1. Introduction

Antimicrobial resistance (AMR) has emerged as a critical global public health threat, necessitating the urgent development of novel, efficacious, and safe antimicrobial agents.[1] Researchers are actively investigating compounds with innovative structural frameworks and alternative mechanisms of action to address AMR challenges. Among these, heterocyclic scaffolds have garnered significant attention in antimicrobial drug discovery due to their

[a]*State Key Laboratory of Green Pesticides, Key Laboratory of Green Pesticide and Agricultural Bioengineering, Ministry of Education, Center for R&D of Fine Chemicals of Guizhou University, Guiyang, 550025, China. E-mail: jhzx.msm@gmail.com; xiangzhou@gzu.edu.cn*

[b]*Bijie Branch of Guizhou Tobacco Company, Bijie, Guizhou 551700, China. E-mail: luozhenbao-1979@163.com*

† Zhaoju Sun, Ting Li, and Yi He contributed equally.

Zhaoju Sun

Zhaoju Sun was born in 2000 in Rizhao, China. She is a master student in State Key Laboratory of Green Pesticide, Key Laboratory of Green Pesticide and Agricultural Bioengineering, Ministry of Education, Center for R&D of Fine Chemicals of Guizhou University, Guiyang, China.

Ting Li

Ting Li was born in 1998 in Guiyang, China. She is a master student in State Key Laboratory of Green Pesticide, Key Laboratory of Green Pesticide and Agricultural Bioengineering, Ministry of Education, Center for R&D of Fine Chemicals of Guizhou University, Guiyang, China.

structural versatility and potent biological activities. In particular, nitrogen-containing heterocyclic compounds have become a focal point in the research and development of antimicrobial drugs.[2–4]

Pyrrolopyrimidines represent a class of nitrogen heterocyclic compounds with substantial pharmacological relevance. Their core scaffold consists of a pyrrole ring covalently linked to a pyrimidine ring.[5,6] To date, five major pyrrolopyrimidine analogs have been identified: pyrrolo[3,2-*d*]pyrimidine, pyrrolo[2,3-*d*]pyrimidine, pyrrolo[1,2-*c*]pyrimidine, pyrrolo[3,4-*d*]pyrimidine, and pyrrolo[1,2-*a*]pyrimidine.[7] Among these, pyrrolo[2,3-*d*]pyrimidines have attracted significant attention due to their structural resemblance to purine nucleotides.[8–13] Known as 7-deazapurines, these compounds belong to the purine metabolite family and can be isolated from diverse natural sources, including terrestrial microorganisms (*e.g.*, soil bacteria) and marine organisms (*e.g.*, red algae).[14–17] These compounds combine the electron-rich nature of pyrrole with the electron-deficient nature of pyrimidine, making them versatile building blocks for synthesis. Through site-selective modification, their biological activity and/or physical properties can be directed and regulated. Pharmacological studies have demonstrated that pyrrolo[2,3-*d*]pyrimidines exhibit multifunctional bioactivities, including antibacterial,[18] antifungal,[19] antiviral,[20,21] antiinflammatory,[22–24] antitumor,[25–29] and kinase inhibitory properties.[30–34] However, while numerous studies focus on their antitumor applications, fewer systematically summarize their antimicrobial potential.

This review aims to systematically evaluate the synthetic methodologies of pyrrolo[2,3-*d*]pyrimidines and synthesize recent advancements in their antimicrobial activities, encompassing antibacterial, antifungal, and antiviral effects. We will critically analyze the advantages and limitations of diverse synthetic strategies and comprehensively discuss reported pyrrolo[2,3-*d*]pyrimidine derivatives with antimicrobial activities. This analysis is intended to provide a theoretical foundation and reference for subsequent drug development, offering new insights and directions for designing more effective and safer antimicrobial agents (Fig. 1).

2. Chemistry synthesis of pyrrolo[2,3-*d*]pyrimidine

2.1 Methodology for the synthesis of pyrrolo[2,3-*d*]pyrimidine

The pyrrolo[2,3-*d*]pyrimidine scaffold has emerged as a focal point in heterocyclic chemistry, with a notable surge in research

Yi He is an administrator in Bijie Branch of Guizhou Tobacco Company, Bijie, Guizhou 551700, China. His research mainly focuses on pest and disease management of crops.

Hongwu Liu is a doctor in State Key Laboratory of Green Pesticides, Key Laboratory of Green Pesticide and Agricultural Bioengineering, Ministry of Education, Center for R&D of Fine Chemicals of Guizhou University, Guiyang, 550025, China.

Linli Yang is a doctor in State Key Laboratory of Green Pesticides, Key Laboratory of Green Pesticide and Agricultural Bioengineering, Ministry of Education, Center for R&D of Fine Chemicals of Guizhou University, Guiyang, 550025, China.

Zhibing Wu is a full professor in State Key Laboratory of Green Pesticides, Key Laboratory of Green Pesticide and Agricultural Bioengineering, Ministry of Education, Center for R&D of Fine Chemicals of Guizhou University, Guiyang, China. His research mainly focuses on design and synthesis of small molecules of pesticides and action mechanisms of highly active molecules.

Liwei Liu is a doctor in State Key Laboratory of Green Pesticides, Key Laboratory of Green Pesticide and Agricultural Bioengineering, Ministry of Education, Center for R&D of Fine Chemicals of Guizhou University, Guiyang, 550025, China.

Zhenbao Luo is an administrator in Bijie Branch of Guizhou Tobacco Company, Bijie, Guizhou 551700, China. His research mainly focuses on pest and disease management of crops.

Xiang Zhou

Xiang Zhou is a full professor in State Key Laboratory of Green Pesticides, Key Laboratory of Green Pesticide and Agricultural Bioengineering, Ministry of Education, Center for R&D of Fine Chemicals of Guizhou University, Guiyang, China. He received his B.Sc. degree in Applied Chemistry from YiLi Normal University in 2014 and PhD degree in 2020 in Pesticide Science from Guizhou University. His research areas include green agrochemical discovery, their structure–activity relationship (SAR) and action mechanisms, and nano-based smart pesticide formulation.

Song Yang

Song Yang is a full professor and director in State Key Laboratory of Green Pesticide, Key Laboratory of Green Pesticide and Agricultural Bioengineering, Ministry of Education, Center for R&D of Fine Chemicals of Guizhou University, Guiyang, China. He received his B.Sc. degree in Chemical Engineering from East China University of Science and Technology in 1995 and received his M.Sc. degree in 2001 and PhD degree in 2005 in Agricultural Pharmacology from Guizhou University. His current research includes organic synthesis methodologies of agrochemicals and functional molecules, agriculture sensing applications, and biomass conversion.

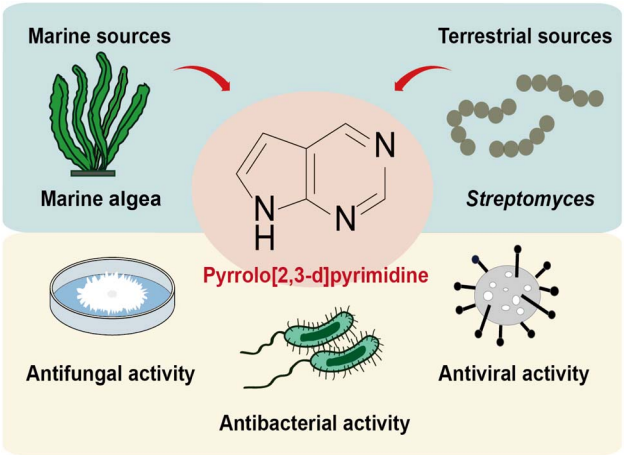

Fig. 1 The main natural sources and antimicrobial activities of pyrrolo[2,3-*d*]pyrimidines.

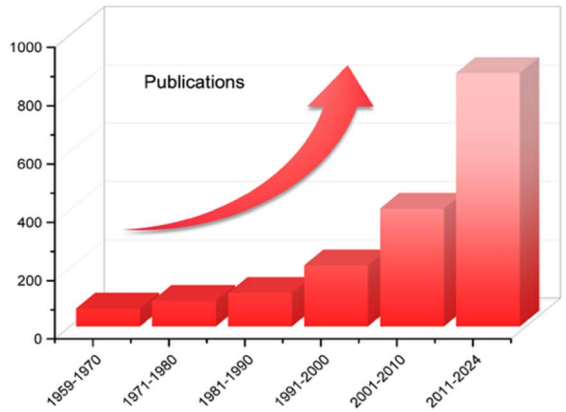

Fig. 2 The number of studies containing the pyrrolo[2,3-*d*]pyrimidine core over the period 1959–2024. Search performed on 10 April 2025 by SciFinder Research Topic using pyrrolo[2,3-*d*]pyrimidine as the keyword.

output from 1990 to 2024 (Fig. 2). According to SciFinder® analytics, pharmacological investigations of these derivatives have significantly outpaced studies on synthetic methodologies, reflecting a strategic emphasis on elucidating their biochemical and therapeutic potential. Two classical annulative strategie do minate the synthetic landscape (Scheme 1): approach A leverages formamides, nitrile derivatives, and esters to construct the pyrrole ring *via* a Paal–Knorr-type cyclization, providing superior regioselectivity for C7-substituted derivatives. In contrast, approach B focuses on pyrimidine ring construction as the key cyclization step through the condensation of appropriately functionalized precursors. These two preparation strategies not only highlight the scaffold's synthetic versatility but also underscore opportunities for developing innovative cyclization pathways.

2.1.1 Synthesis by formation of the pyrimidine ring

2.1.1.1 From a pyrroloring containing an amide bond. In 2010, Davoodnia *et al.* developed a cyclocondensation protocol

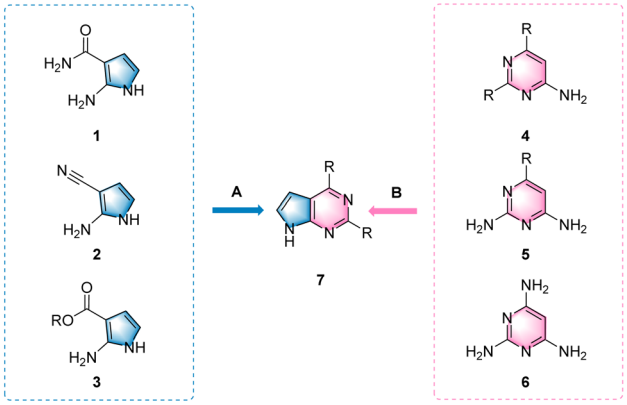

Scheme 1 Two classical methods for the synthesis of pyrrolo[2,3-*d*]pyrimidine scaffolds. (A) Ring closure by the formation of the pyrimidine; (B) ring closure by the formation of pyrrolo.

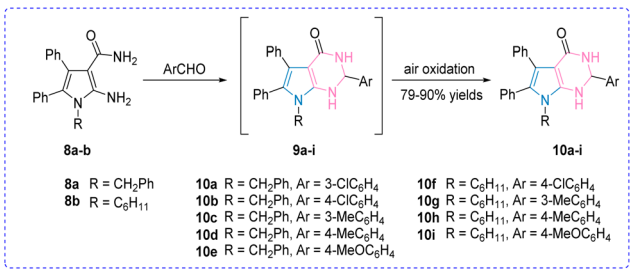

Scheme 2 Catalytic synthesis of new pyrrolo[2,3-*d*]pyrimidine-4-ones with Brønsted-acidic ionic liquid.

between 2-amino-1*H*-pyrrole-3-carboxamide derivatives (**8a–b**) and aromatic aldehydes under solvent-free conditions.[35] Utilizing the Brønsted-acidic ionic liquid $[(CH_2)_4SO_3HMIM][HSO_4]$ as catalyst with air oxidation at 85 °C, this method efficiently produced 2-aryl-3,7-dihydro-4*H*-pyrrolo[2,3-*d*]pyrimidine-4-ones (**10a–i**) in good yields, though the proposed intermediates (**9a–i**) could not be isolated (Scheme 2).

Building upon this foundation, Frolova's group introduced in 2013 an alternative three-component strategy employing sulfonamides, aromatic aldehydes, and cyanoacetamide.[36] Their K_2CO_3-catalyzed synthesis generated aminopyrroles (**15a–c**), which subsequently underwent carbonylative cyclization with oxalyl chloride in diglyme to yield structurally diverse pyrrolo[2,3-*d*]pyrimidine-2,4-dione analogs (**16a–c**) (Scheme 3).

2.1.1.2 From a pyrroloring containing a carbon and nitrogen triple bond. In 1998, Dave *et al.* synthesized 5,7-disubstituted 4-amino-7*H*-pyrrolo[2,3-*d*]pyrimidine *via* the Gewald reaction. The two-step process began with the reaction of (2-bromo-1-arylalkylidene)propanedinitriles **17** and various fluorinated aromatic amines, which generated 1,4-disubstituted 2-amino-3-cyanopyrrole **18**. Subsequently, compound **18** underwent cyclocondensation with formamide in *N*,*N*-dimethylformamide (DMF); notably, the addition of a small amount of formic acid significantly improved the yield of **19**.[37,38] Mechanistically, this transformation likely involves the partial hydrolysis of the cyano

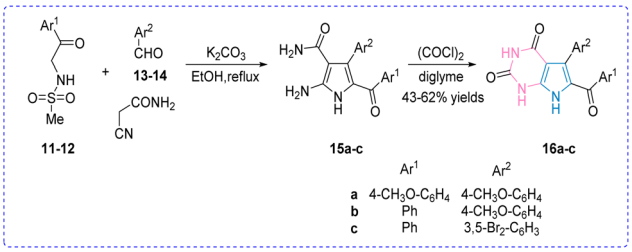

Scheme 3 A multicomponent reaction based synthesis of pyrrolo[2,3-*d*]pyrimidine-2,4-dione analogs.

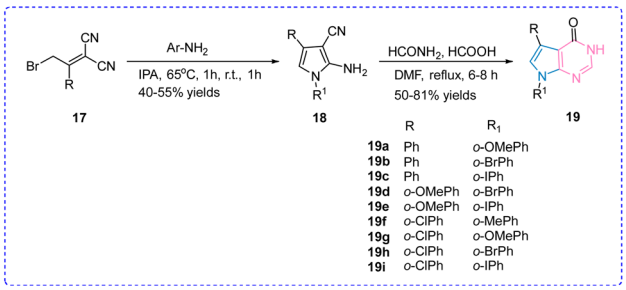

Scheme 4 Preparation of 5,7-disubstituted 4-amino-7*H*-pyrrolo[2,3-*d*]pyrimidines using the Gewald reaction.

group at position **19** of **18**, resulting in the formation of an intermediate amide, which then undergoes intramolecular cyclization to furnish the final product (Scheme 4).

In 2000, Hess and colleagues developed a two-step synthetic protocol to access pyrrolo[2,3-*d*]pyrimidine derivatives.[39] The methodology commenced with the condensation of *o*-amino-pyrrolocarbonitrile **20** and acyl chloride **21**, forming amide intermediate **22**. Subsequent treatment with phosphorus pentoxide in a DMF/water mixed solvent system at elevated temperature (190 °C) achieved cyclization to afford pyrrolo[2,3-*d*]pyrimidine **23a–e**, with structural diversity introduced through nucleophilic substitution using various amino derivatives (Scheme 5).

In 2011, Xiao *et al.* synthesized several arylated derivatives of xylocydine **24**.[40] This natural nucleoside is a nanoscale CDK inhibitor. Pyrrolo **26** was synthesized in HBr and acetic acid

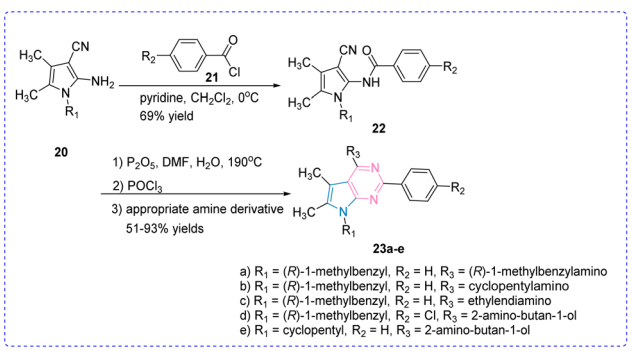

Scheme 5 Synthesis of pyrrolo[2,3-*d*]pyrimidines using *o*-amino-pyrrolidine cyanide.

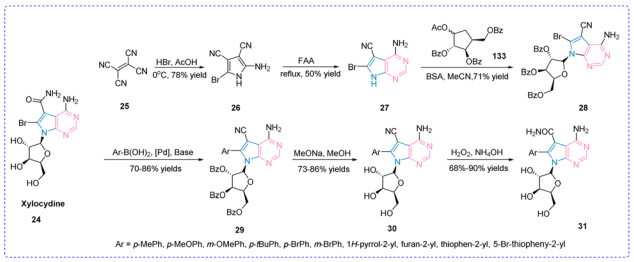

Scheme 6 Synthesis of 6-(heptyl)aryl lignocaine analogs.

using tetracyanoethylene **25** as a raw material. Condensation with formamidine gave pyrrolo[2,3-*d*]pyrimidine **27**. Protection of xylofuranose **28**, starting with (-)-xylose, was used to glycosylate **26**, providing **28**. Depending on the nature of the aryl group, different conditions were used to complete the Suzuki coupling, resulting in good yields of compound **29**. Compound **30** was obtained by deprotection by treatment with sodium methanol and final synthesis of the nitrile into an amide to give arylated xylocydines **30**. The amide compound **31** was inactive against CDK1 and CDK2, while the thiophene-2-yl- and furan-2-yl-substituted cyano-analogs **31** showed single-digit μm activity against CDK2 (Scheme 6).

2.1.1.3 From pyrroloring containing an ester group. In 2001, Taylor *et al.* developed a 4-dimethylaminopyridine-catalyzed radical cyclization of various *N*-substituted malondiamides **32** using manganese triacetate/copper acetate to generate pyrrolo-containing malondiamides **33**.[41] The resulting 2-amino-4(3*H*)-pyrimidinone cycloguanidine was further cyclized to 3-methoxy-2-pyrrolidinone **34**, which served as a substrate for a palladium-catalyzed Heck reaction (Scheme 7).

In 2006, Pittalà *et al.* developed a multistep synthesis of pyrrolo[2,3-*d*]pyrimidines through sequential functionalization. The process initiated with amino ester derivatives (**35–41**) undergoing urethane formation with 2-chloroethyl isocyanate in refluxing toluene.[42] Subsequent coupling with substituted piperazines in tetrahydrofuran (THF) ($NaI/NaHCO_3$) generated intermediates, which underwent alkaline methanolysis to afford final derivatives **49a–n** in 85–98% yields (Scheme 8).[43]

In 2011, Kaspersen *et al.* developed a four-step synthetic route to access 4-hydroxypyrrolo[2,3-*d*]pyrimidines. Initial treatment of ethyl cyanoacetate (**50**) with HCl-saturated ethanol yielded crystalline precursor **51**, whose subsequent free base liberation (aqueous K_2CO_3, 0 °C) enabled ammonium chloride-

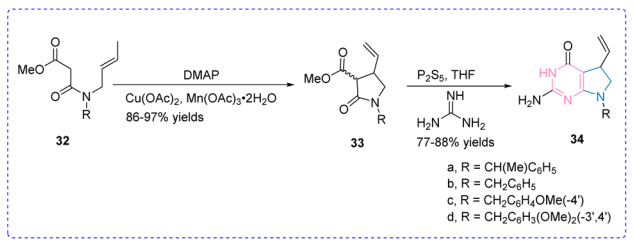

Scheme 7 Synthesis of pyrrolo[2,3-*d*]pyrimidines using DMAP-catalysed radical cyclization.

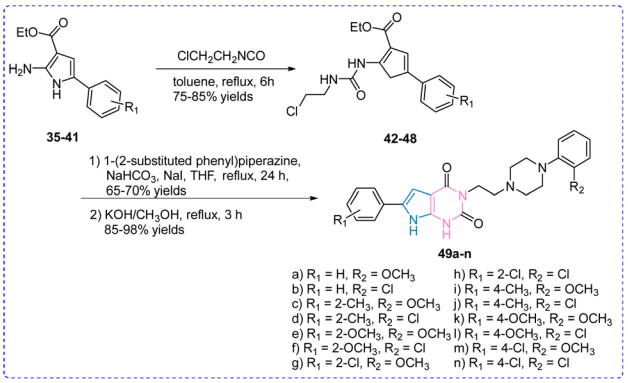

Scheme 8 Synthesis of pyrrolo[2,3-*d*]pyrimidines using amino ester pyrroles.

mediated conversion to ethyl 3-amino-3-iminopropionate hydrochloride (**52**) under ethanol reflux. Following a reported protocol,[1] sodium ethoxide-promoted alkylation of **52** with α-bromoacetophenones proceeded under divergent thermal conditions – ambient temperature (12 h) *versus* 60 °C (1.5–3 h) delivering pyrrolidine intermediates **53a–e** in 48–64% yields after purification. Although not systematically investigated, the moderate yields were postulated to originate from inherent instability analogous to 2-amino-3-ethoxycarbonylpyrrole derivatives. The synthetic sequence culminated in formamide-induced cyclization of **53a–e** within a formic acid/DMF system, followed by 2-propanol precipitation to isolate target compounds **54a–e** with improved yields (54–74%, Scheme 9).

2.1.1.4 From urea/guanidine derivatives. In 2008, Mizar *et al.* developed an efficient Biginelli-type synthesis of pyrrolo[2,3-*d*]pyrimidines **58a–e** through a three-component domino condensation.[44] Employing 1-methylpyrrolidinone (**55**) as the heterocyclic core, aryl aldehydes (**56**) as carbonyl donors, and urea/guanidine derivatives (**57**) as nitrogen sources, the KF–Al_2O_3-mediated reaction in ethanol at 80 °C (3–5 h) delivered target compounds with good to excellent yields, as illustrated in Scheme 10.

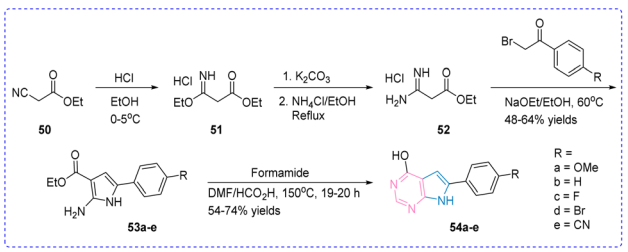

Scheme 9 Synthetic route to the 4-chloropyrrolopyrimidines **50–54**.

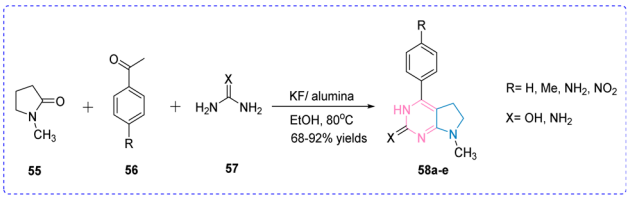

Scheme 10 Preparation of pyrrolo[2,3-*d*]pyrimidines by the Biginelli reaction, a three-component condensation reaction.

2.1.2 Synthesis by the formation of the pyrroloring

2.1.2.1 From pyrimidine. In 2006, Choi *et al.* developed a three-step protocol for constructing pyrrolo[2,3-*d*]pyrimidine derivatives through sequential functionalization.[45] The synthesis commenced with 5-bromo-2,4-dichloropyrimidine (**59**) undergoing regioselective amination at the C4 position *via* optimized nucleophilic substitution in ethanol reflux, yielding 6-amino intermediate **60** with 96% efficiency. Subsequent Stille cross-coupling of 60 with vinylstannane under $Pd(PPh_3)_4$ catalysis in THF (60 °C, 12 h) delivered vinyl ether **61**. Final HCl-mediated cyclization (1 M, 80 °C) completed the annulation process, generating target scaffold **62** with full structural confirmation by 2D-Nuclear Magnetic Resonance (NMR) (Scheme 11).

In 2009, Nagashima *et al.* obtained a 2-aniline derivative by substituting 1,6-dihydro-2-methyl-thio-6-oxy-5-pyrimidine methyl ester **63** with 4-morpholine aniline.[46] A 2-aniline derivative is chlorinated with phosphorus trichloride in the presence of diethylaniline to obtain a 4-chlorinated derivative **64**. The synthetic pathway commenced with nucleophilic displacement of the C4-chloride group using benzylamine to generate the 4-benzylamino derivative. Sequential hydrolysis of the intermediate provided the carboxylic acid precursor, which underwent amidation with *N*,*O*-dimethylhydroxylamine to furnish the *N*-methoxy-*N*-methyl carboxamide derivative. Reduction of this intermediate with lithium aluminum hydride yielded aldehyde derivatives **65a–d** in 53–82% yields. These aldehydes were subjected to Wittig olefination using (methoxymethyl)triphenylphosphonium chloride, followed by acidic cyclization (HCl/MeOH) to afford the target pyrrolo[2,3-*d*]pyrimidine derivatives **66a–d** (Scheme 12).

In 2013, El Kaïm *et al.* extended the synthesis of 5,6-disubstituted pyrrolo[2,3-*d*]pyrimidine derivatives through a four-component Ugi–Smiles reaction between ancymidol **67** and nitroolefins, yielding intermediates **68** in low-to-moderate yields.[47] Subsequent Sonogashira coupling followed by base treatment (*e.g.*, K_2CO_3) efficiently generated target compounds **69** or **70** in 65–82% yields. When aromatic aldehydes were employed, the Ugi adducts and Sonogashira products could be isolated separately or synthesized *via* a one-pot protocol;

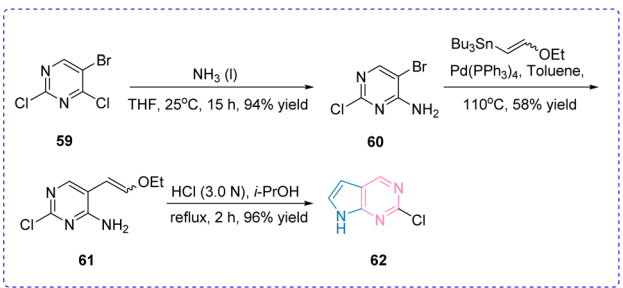

Scheme 11 Synthesis of 2-chloropyrrolo[2,3-*d*]pyrimidines.

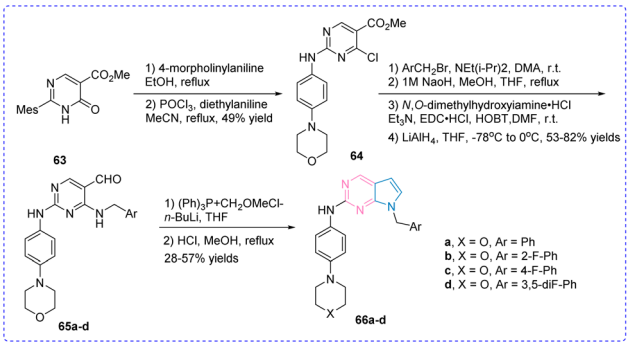

Scheme 12 Synthesis of pyrrolo[2,3-*d*]pyrimidines using the Wittig reaction.

however, reactions with formaldehyde (R_1 = H) required stronger bases such as NaH at room temperature due to the reduced acidity of the *ortho*-proton. The final cyclization of intermediate **71** exhibited pronounced substituent-dependent regioselectivity, succeeding with phenyl, *ortho*/*para*-chlorophenyl, or *para*-fluorophenyl groups (R_2) yet failing completely for electron-rich arenes (*para*-methylphenyl, *para*-methoxyphenyl) in the presence of aliphatic aldehydes (R_1 = alkyl). Intriguingly, certain substrates underwent an unexpected divergent cyclization pathway to form pyrrolo[2,3-*d*]pyrimidine **72**, suggesting benzyl residue activation as a key mechanistic driver (Scheme 13).

2.1.2.2 From aminopyrimidine. In 2000, Rodriguez *et al.* successfully synthesized intermediate **74** through a Sonogashira coupling reaction between 4,6-dimethyl-2-amino-3-halogenated pyrimidine (substrate **73**) and 1-alkyne under palladium catalysis (Pd), achieving excellent yields.[48] Subsequently, intermediate **74** underwent base-mediated cyclization in *N*-methylpyrrolidone (NMP) solvent at ambient temperature (25 °C) using potassium *tert*-butoxide (*t*-BuOK) as the base, yielding pyrrolo[2,3-*d*]pyrimidine derivative **75** in 61% isolated yield (Scheme 14).

In 2011, Aso *et al.* employed an analogous strategy to synthesize 5-bromo-2-(dipropylamino)pyrrolo[2,3-*d*]pyrimidin-4-one **78** through the reaction of 2-amino-4-hydroxy-6-(methylamino)pyrimidine **76** with 1-chloro-2-propanone.[49]

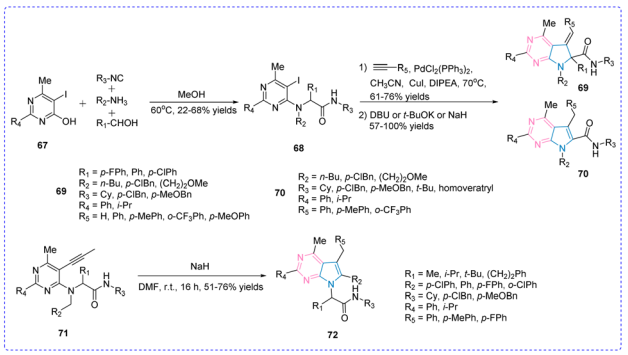

Scheme 13 Preparation of pyrrolo[2,3-*d*]pyrimidines by the Ugi–Smiles reaction, a four-component condensation reaction.

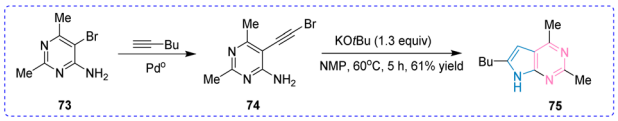

Scheme 14 Synthesis of pyrrolo[2,3-*d*]pyrimidine derivatives using Sonogashira reaction.

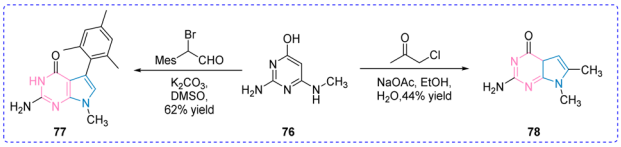

Scheme 15 Synthesis of pyrrolo[2,3-*d*]pyrimidin-4-one derivatives.

Notably, the authors achieved regioselective substitution at the 5-position of intermediate **77** by reacting **76** with 2-bromo-2-(mesityl)acetaldehyde, demonstrating the synthetic versatility of this protocol (Scheme 15).

In 2012, Paul *et al.* reported a catalytic synthesis of 5-arylpyrrolo[2,3-*d*]pyrimidine-2,4-diones (**81**) through the reaction of 6-aminouracil (**79**) with nitroolefins (**80**) using polyethylene glycol-supported sulfonic acid (PEG–SO_3H) as a polymer-supported Brønsted acid catalyst.[50] The reaction achieved high yields (75–92%), with substrates bearing electron-donating groups on the aromatic ring exhibiting optimal performance. Notably, the requisite nitroolefins were generated *in situ* from uracil (**82**) and aromatic aldehydes in nitromethane, catalyzed by magnetically recoverable copper ferrite ($CuFe_2O_4$) nanoparticles. This bifunctional catalyst enabled efficient cyclization while allowing simple separation *via* external magnetic fields, demonstrating excellent recyclability over five cycles (Scheme 16).

In 2016, Saikia *et al.* developed a one-pot two-step protocol for synthesizing pyrrolo[2,3-*d*]pyrimidine derivatives **86a–k** (42–92% yield) through sequential Michael addition and reductive cyclization.[51] The reaction commenced with 6-amino-1,3-dimethylpyrimidine-2,4(1*H*,3*H*)-dione (**84**) and (*E*)-β-nitrostyrene (**85**) in ethanol under alkaline conditions (NaOH, 2 h, 25 °C), followed by intermediate structural confirmation through single-crystal X-ray analysis. Subsequent treatment of the Michael adduct with a $Na_2S_2O_4$/NaOH/EtOH system (1 : 3 : 4 molar ratio) at 60 °C for 1 h triggered reductive cyclization to furnish the target compounds. This strategy effectively

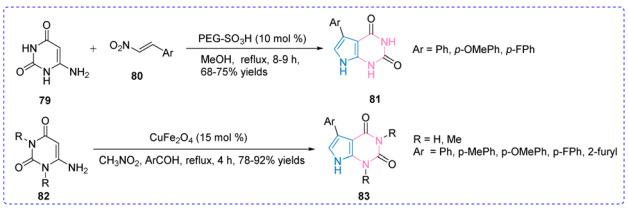

Scheme 16 Synthesis of 5-arylpyrrolo[2,3-*d*]pyrimidines: the catalyst can be easily recovered by an external magnet.

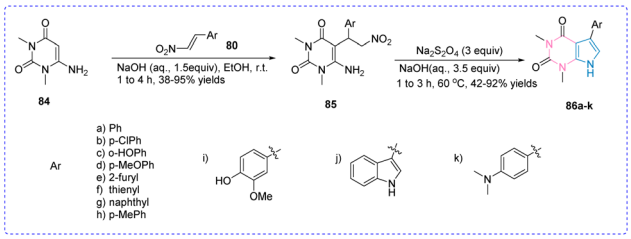

Scheme 17 A one-pot, two-step synthesis of 5-arylpyrrolo[2,3-*d*]pyrimidines.

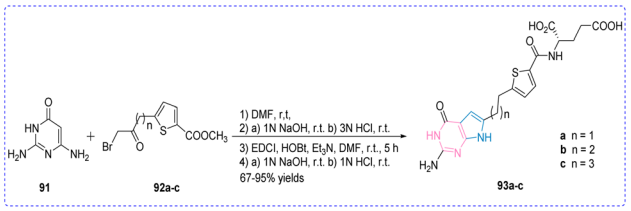

Scheme 19 Synthesis of pyrrolo[2,3-*d*]pyrimidines containing thiophene groups.

leveraged the dual advantages of alkaline sodium dithionite's strong reducing capacity and Michael addition compatibility in basic media, enabling efficient construction of the pyrrolo[2,3-*d*]pyrimidine core (Scheme 17).

In 2021, Tan *et al.* established a synthetic pathway for pyrrolo[2,3-*d*]pyrimidine derivatives through sequential transformations.[52] The protocol commenced with 6-aminouracil (**79**) undergoing cyclization with chloroacetaldehyde in acetate buffer (pH 4.5, 80 °C), yielding pyrrolo[2,3-*d*]pyrimidine-2,4-diol (**87**) in 93% isolated yield. Subsequent treatment of **87** with phosphorus oxychloride ($POCl_3$, DMF catalyst) under reflux (110 °C, 4 h) achieved complete chlorination to afford 2,4-dichloro-7*H*-pyrrolo[2,3-*d*]pyrimidine (**88**) Compound **88** then underwent consecutive nucleophilic substitutions: first with *N*-[3-(aminomethyl)pyridin-2-yl]-*N*-methylmethanesulfonamide in ethanol under reflux conditions, followed by microwave-mediated coupling (150 °C, 300 W, 45 min) with 5-aminoindol-2-one. This tandem process efficiently produced hybrid compound **90**, demonstrating successful integration of dual bioactive moieties through sequential functionalization (Scheme 18).

2.1.2.3 From diaminopyrimidine. In 2011, Wang *et al.* adapted the aforementioned methodology to synthesize 2-amino-4-yloxy-6-substituted pyrrolo[2,3-*d*]pyrimidines through a bromoketone-mediated pathway.[53] The synthesis involved reacting α-bromoketones **92a–c** with 2,6-diamino-3*H*-pyrimidin-4-one (**91**) under ambient conditions (room temperature, 72 h) in DMF, followed by alkaline hydrolysis (1 N NaOH, room temperature) of the intermediate products to afford carboxylic acid derivatives **93a–c** in 89–95% isolated yields. This two-stage protocol demonstrated remarkable functional group tolerance while maintaining reaction efficiency, as systematically illustrated in Scheme 19.

In 2013, Shi *et al.* treated **91** with chloral aqueous solution to produce pyrrolo[2,3-*d*]pyrimidine **95**.[54] By performing this cyclization in the presence of *N*,*N*-dimethylacetamide (DMA) rather than DMF, the required product is precipitated as a 1 : 1 DMA complex **94**, which facilitates its production on a kilogram scale. 95% DMA is then easily removed by recrystallization from MeOH. PivCl was used to protect the amino group to obtain amide **96**. Deoxychlorination was best achieved with the $POCl_3$/$BnEt_3NCl$ system to obtain **97**, followed by iodization with *N*-iodosuccinimide (NIS) to obtain **98** regionally. It is important to note that neopentyl groups are necessary for the successful process of deoxychlorination and iodization. Attempts to replace neopentyl groups with acetyl or octyl groups result in complex mixtures of products when treated sequentially with $POCl_3$ and NIS. However, cutting the neopentyl group proved to be a difficult operation. After extensive experiments, we found that if **100** was first alkylated with commercially available chloromethyl pyridine **99** and then treated with $ZnCl_2$ in EtOH to obtain the key intermediate **101**, the neopentyl group could be effectively removed and performed **102** (Scheme 20).

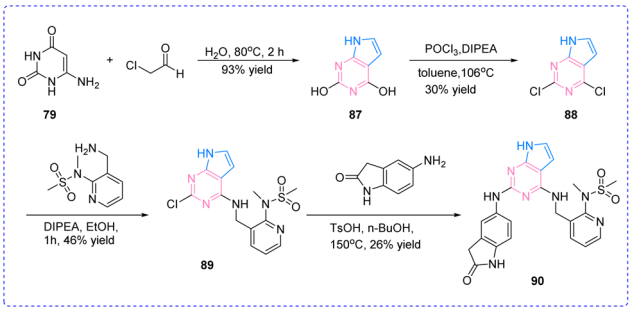

Scheme 18 Synthetic route for 7*H*-pyrrolo[2,3-*d*]pyrimidine derivative.

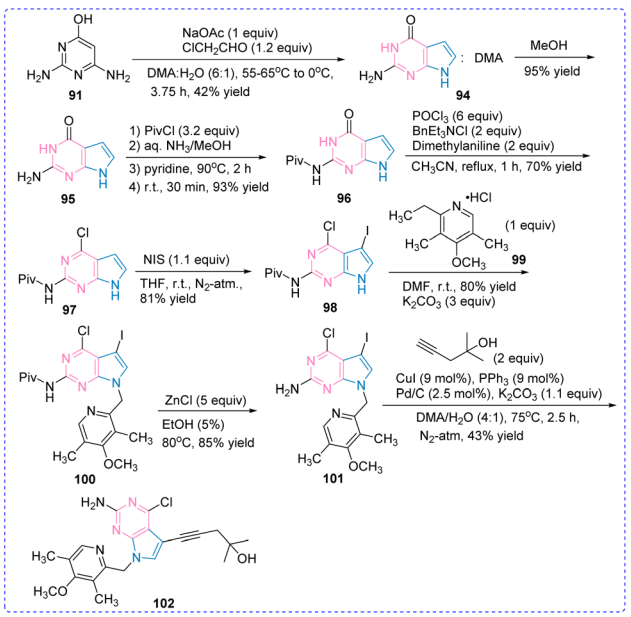

Scheme 20 Synthesis of pyrrolo[2,3-*d*]pyrimidines containing an alkynyl group.

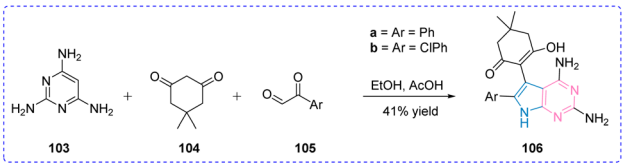

Scheme 21 Synthesis of pyrrolo[2,3-*d*]pyrimidines using a three-component condensation reaction.

2.1.2.4 From pyrimidinetriamine. In 2010, Quiroga *et al.* carried out a three-component reaction of 2,4,6-pyrimidinetriamine **103**, acetone **104**, and arylglyoxals **105** at 242–281 °C, affording compounds **106a** and **106b** in 41% combined yield (Scheme 21).[55]

In 2014, Khalaf *et al.* developed a regioselective synthesis of 4-amino-5,6-diarylpyrrolo[2,3-*d*]pyrimidines through bromoketone-mediated cyclization. The protocol employed 2,4,6-pyrimidinetriamine (**103**) and pre-synthesized diaryl α-bromoketones prepared *via* bromination of aryl methyl ketones (commercially sourced or obtained through Friedel–Crafts acylation of substituted benzenes)—under optimized coupling conditions (DMF, 100 °C, 12 h).[56] Despite systematic optimization, the condensation reaction furnished 5,6-diaryl pyrrolo pyrimidines **107a–j** in modest yields (Scheme 22).

2.1.3 Synthesis of another method. An alternative synthetic strategy employs the inverse electron-demand Diels–Alder (IEDDA) reaction between 2,4,6-triazine derivatives (**108**) and *N*-alkylated-2-aminopyrroles (**109**).[57] This cascade process initiates with the formation of cycloadduct **111**, which undergoes retro-Diels–Alder elimination of nitrile at 60 °C (DMF, 12 h). The liberated nitrile undergoes nucleophilic attack by the pyrrole's free amino group to form amidinium intermediate **112** in high yield. The system accommodates diverse substituents (alkyl, benzyl, thioether), while electron-withdrawing groups (esters, trifluoromethyl groups) dramatically enhance triazine reactivity, allowing ambient-temperature reactions *versus* mandatory heating for unactivated substrates (Scheme 23).

In 2005, Janeba *et al.* developed two synthetic routes to access pyrrolo[2,3-*d*]pyrimidine derivatives **115**.[58] The stepwise approach first employed **113a–b** in a Sonogashira coupling with terminal alkynes using $Pd(PPh_3)_4$/CuI catalysis in DMF/triethylamine (70 °C, 12 h), yielding intermediates **114** (51–83%). Subsequent treatment of **114** with methanolic ammonia (7 M, 70 °C, 8 h) afforded 6-alkyl-3-[(2-hydroxyethoxy)methyl] pyrrolo[2,3-*d*]pyrimidine-2(3*H*,7*H*)-ones **115** (53–84%). Alternatively, a one-pot protocol directly converted **113a**/**b** to **115** through sequential palladium-mediated coupling (60 °C, 8 h) and *in situ* cyclization, followed by silica gel chromatography and NH_3/MeOH treatment to achieve simultaneous deacetylation and furan-to-pyrrolo ring transformation, albeit with reduced yields (30–53%) (Scheme 24).

In 2012, Davies and colleagues first synthesized 2-bromo-1,1-diethoxyethane **116** and ethyl-2-cyanoacetate **117** in DMF at 90 °C using Bu_4NBr and K_2CO_3 as catalysts.[59] The intermediate (**118**) was obtained with a yield of 40–55%. Subsequently, 2-cyano-4,4-ethoxybutyrate (**118**) reacted with thiourea under alkaline conditions to produce pyrimidine (**119**) with a yield of 50%. Following sulfhydryl methylation, acid-mediated ring closure yielded pyrrolo[2,3-*d*]pyrimidine (**120**) scaffolds in excellent yield. Deoxychlorination using phosphorus oxide trichloride and silyl ethyl methyl (SEM) protection of the pyrrole nitrogen proceeded with good yields. To introduce a cyano group at C5, the C5 site was brominated using *N*-bromosuccinimide. Lithium–halogen exchange with butyllithium followed by quenching with carbon dioxide afforded carboxylic acid (**127**) in excellent yield. The acid was further converted into an acyl chloride using oxaloyl chloride, which subsequently reacted with aqueous ammonia to produce amide (**128**) with high yield. Suzuki coupling of the C5 position with a cyano

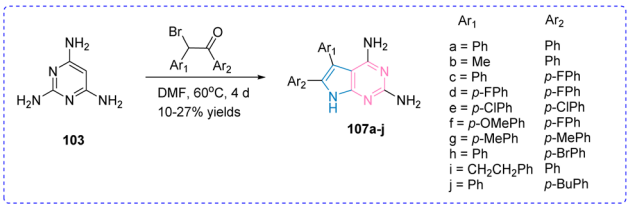

Scheme 22 Synthesis of pyrrolo[2,3-*d*]pyrimidines using two pyrimidine substrates.

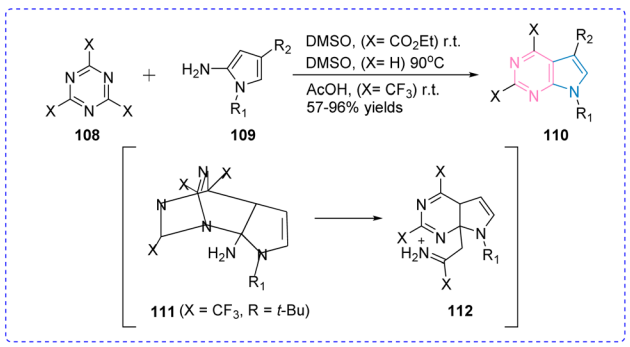

Scheme 23 Synthesis of pyrrolo[2,3-*d*]pyrimidines using the Diels–Alder reaction.

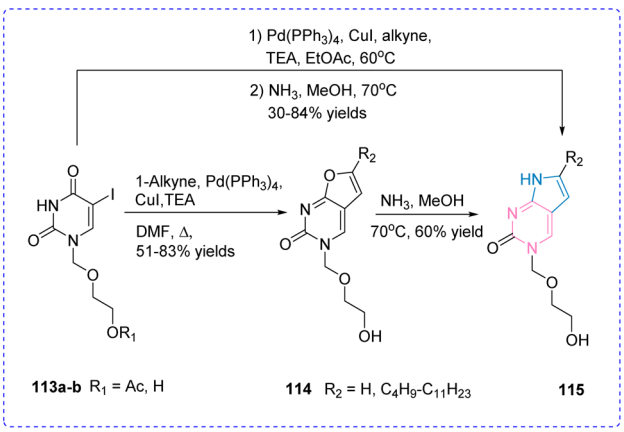

Scheme 24 Synthesis of pyrrolo[2,3-*d*]pyrimidines *via* one-pot coupling.

group oxidized the sulfide to sulfone using *m*-chloroperbenzoic acid. Under alkaline conditions, the sulfone was replaced by ethyl thioglycolate with excellent yield, and carboxylic acid (**127**) was obtained quantitatively *via* saponification with sodium hydroxide. This acid was then converted into amido (**128**) in an *O*-(benzotriazol-1-yl)*N*,*N*,*N*′,*N*′-tetramethyluronium hexafluorophosphate mediated reaction. Using pyridine *p*-toluene sulfonate (PPTS) as a weak acid catalyst, the acetal functional groups on aryl substituents were decomposed. The deprotected hydroxyl was alkylated with methyl iodide or ethyl iodide, and the SEM group was finally removed using tetrabutylammonium fluoride (TBAF) and ethylenediamine. Compound (**130**) was obtained at a moderate yield (Scheme 25).

In 2013, Tari *et al.* utilized methyl cyanoacetate (**131**) to react with bromobutanone (**132**), forming an acetal to produce compound (**133**) with excellent yield.[60] High-yield pyrimidone was obtained through treatment with urea or thiourea. Acid-catalyzed cyclization of thioanalog (**134**) yielded the first key intermediate (**135**) with excellent yield. Oxygen analogues were similarly treated and subsequently activated with $POCl_3$ to obtain the second key intermediate (**136**) (Scheme 26).

In 2012, Lee *et al.* reported a solid-phase synthesis of pyrrolo[2,3-*d*]pyrimidine derivatives utilizing Rink amide MBHA resin as the polymeric support.[61] The resin was pre-conditioned by swelling in *N*,*N*-dimethylformamide for 2 hours within a syringe reactor, followed by sequential deprotection with 20% piperidine/DMF (2 × 10 minutes) to remove the Fmoc protecting group. Two peptide-like residues were introduced *via* a microwave-assisted submonomer protocol: bromoacetic acid

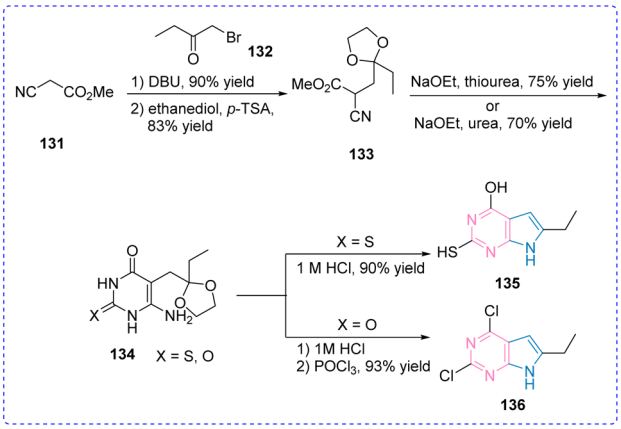

Scheme 26 Formation of pyrrolo[2,3-*d*]pyrimidines *via* acetal intermediates.

and *N*,*N*-diisopropylcarbodiimide (DIC) were sequentially coupled to the resin under DMF, followed by microwave irradiation (10% power, 2 × 15 seconds) with manual bead agitation between pulses to ensure uniformity. After expelling the reaction mixture, the resin was thoroughly washed with DMF, CH_2Cl_2 and MeOH. This microwave-driven coupling cycle was repeated using various amines to yield dimeric peptides (**139**), which were subsequently reacted with 4,6-dichloro-2-(methylthio)pyrimidine-5-carbaldehyde to afford intermediates (**140a–b**). The dicyclopyrrolopyrimidine core (**141a–h**) was constructed *via* intramolecular aldol condensation and *N*,*N*-dimethylation at the 4-position, followed by oxidation of the thioether moiety with *m*-chloroperbenzoic acid (MCPBA) and final amine substitution to generate the 2,6,7-trisubstituted pyrrolo[2,3-*d*]pyrimidine scaffold (**142**) (Scheme 27).

Ryzhkova and coworkers developed a catalyst-free green synthetic protocol for constructing pyrrolo[2,3-*d*]pyrimidine derivatives (**146a–h**) bearing barbituric acid moieties through an aqueous multicomponent reaction. This methodology employs phenylglyoxal (**143**), *N*,*N*′-dimethylbarbituric acid

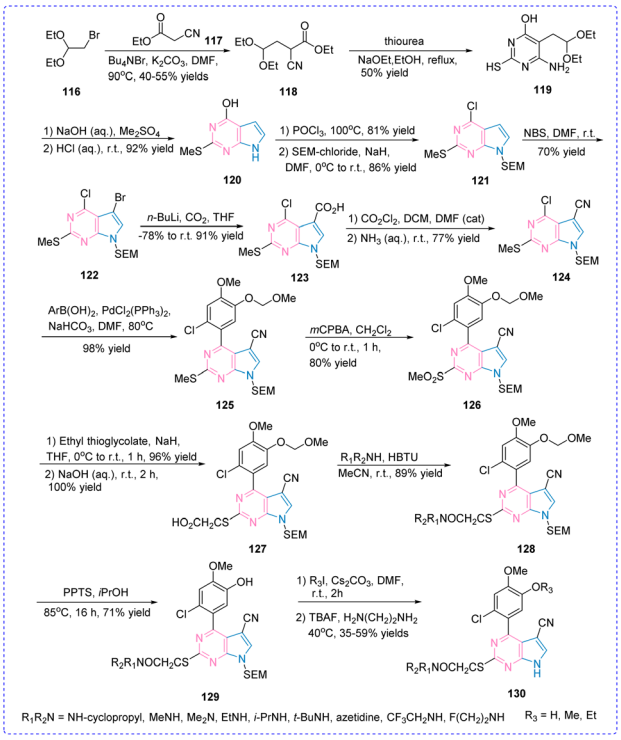

Scheme 25 Synthesis of pyrrolo[2,3-*d*]pyrimidines *via* Suzuki coupling reaction.

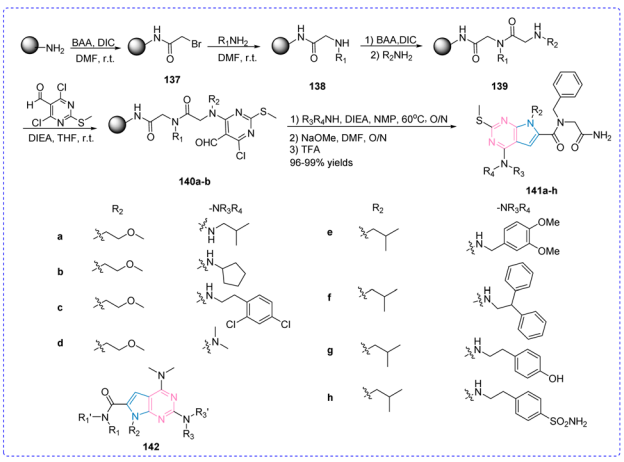

Scheme 27 Synthesis of tetrasubstituted pyrrolo[2,3-*d*]pyrimidines using solid phase synthesis.

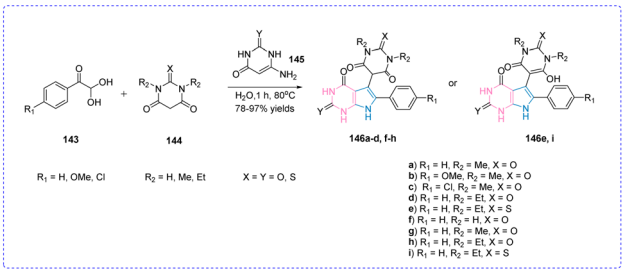

Scheme 28 Novel green on-water multicomponent approach for the synthesis of pyrrolo[2,3-*d*]pyrimidines.

(**144**), and 6-aminouracil (**145**) as starting materials, mechanistically proceeding through sequential Knoevenagel condensation, Michael addition, and intramolecular heterocyclization.[62] Remarkably, the reaction demonstrates exceptional efficiency in pure aqueous medium without requiring catalytic additives. Systematic optimization afforded various target compounds in 78–97% yields. Characterized by operational simplicity and easy product isolation (Scheme 28), this water-based approach aligns with green chemistry principles while providing efficient access to pharmacologically relevant heterocyclic frameworks.

3. Antimicrobial application

Pyrrolo[2,3-*d*]pyrimidines, as structurally unique nitrogen-containing heterocyclic compounds, have garnered significant interest in antimicrobial research owing to their diverse biological activities and high structural adaptability. Representative examples of their antibacterial, antifungal, and antiviral applications are outlined below.

3.1 Antibacterial activity

In 2002, Dave *et al.* synthesized two annulated pyrrolo[2,3-*d*] pyrimidine derivatives incorporating triazole and tetrazole moieties.[63] Tetrazolo-pyrrolo[2,3-*d*]pyrimidines (**148**) were synthesized by treating compound **149** with sodium azide and ammonium chloride in dimethyl sulfoxide (DMSO), whereas triazolo derivatives were obtained through reaction of **154** with heated formic acid. An alternative synthetic pathway involved 2-amino-3-cyanopyrroles (**150**): treatment with triethyl orthoformate yielded intermediates (**151**), which were subsequently condensed with hydrazine hydrate to afford 5,7-disubstituted-3-amino-4-imino-pyrrolo[2,3-*d*]pyrimidines (**152**). Antimicrobial evaluation *via* agar plate diffusion assay against six bacterial strains (*E. coli*, *E. enterica*, *P. aeruginosa*, *S. typhi*, *S. aureus*, *B. subtilis*) demonstrated that most derivatives exhibited comparable activity to reference standards against *E. coli* (with exceptions of **148e** and **148j**). Compound **153** displayed superior potency. Against *E. enterica*, derivatives **148c** and **148k** showed reduced efficacy relative to ampicillin, while others surpassed the control. All compounds exhibited similar activity against *P. aeruginosa*, except **148g**, **148k**, and **153d**, which showed no inhibition. Notably, **148h** and **148k** exceeded the positive

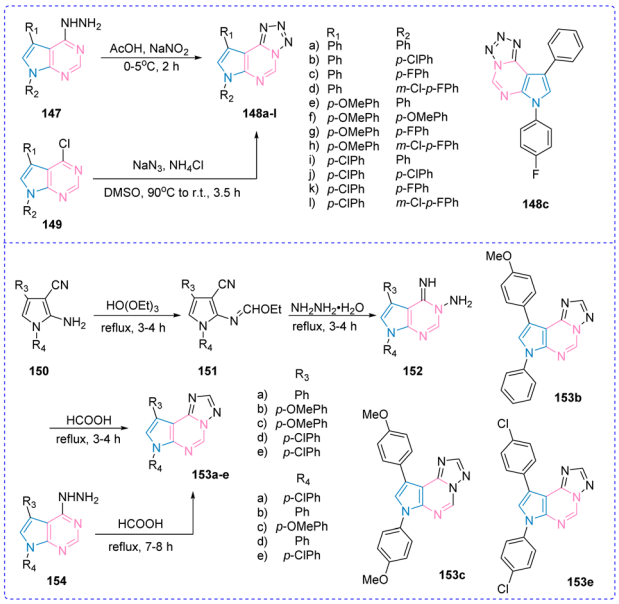

Scheme 29 Synthesis of two cyclized pyrrolo[2,3-*d*]pyrimidines containing triazole and tetrazole.

Table 1 The inhibition zone diameter method was used to determine the antibacterial activity of compounds **148c**, **153b**, **153c**, and **153e**

Compd	Bacteria	Inhibition zone diameter (mm)
148c	*E. coli*	15
	E. enterics	15
	P. aeruginosa	15
	S. typhi	15
	B. subtilis	5
153b	*P. aeruginosa*	15
153c	*B. subtilis*	10
153e	*B. subtilis*	10

control's efficacy against *S. aureus*, whereas **153c** and **153d** demonstrated enhanced activity against *B. subtilis* (Scheme 29 and Table 1).

In 2008, Ghahremanzadeh *et al.* established an environmentally benign synthetic protocol for spiro-pyrrolopyrimidine derivatives through aqueous-phase cyclocondensation.[64] This methodology exploited water's immiscibility with organic reactants to achieve efficient phase separation and catalyst recovery, combining operational simplicity with reduced ecological footprint while maintaining high product yields (Scheme 30). Antimicrobial assessment identified compounds

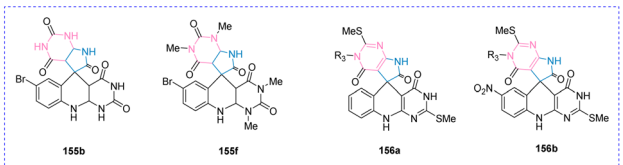

Scheme 30 Structure of compounds **155b**, **155f**, **156a** and **156b**.

155b, **155f**, **156a**, and **156b** as superior to norfloxacin, with **155b** exhibiting a minimum inhibitory concentration (MIC) of 9 μg mL^{-1} against *P. aeruginosa* (*cf.* norfloxacin: 20 μg mL^{-1}) and **156a** demonstrating 7 μg mL^{-1} efficacy against *S. aureus* (*cf.* norfloxacin: 16 μg mL^{-1}). Notably, compound **155f** displayed exceptional antimicrobial potency (Table 2).

Interestingly, in 2010, Mohamed *et al.* devised multifunctional synthetic pathways for pyrrolo[2,3-*d*]pyrimidine derivatives.[65] Initial synthesis of pyrrolo[2,3-*d*]pyrimidine-2/4-thione derivatives (**158**) from precursor **157** was followed by base-mediated alkylation (NaOH/EtOH) to generate pyrrolo[2,3-*d*]pyrimidine (**159**), while condensation routes yielded 2-amino-pyrrolo[2,3-*d*]pyrimidines (**160**) (Scheme 31). Subsequent annulation strategies produced 8-aryl-substituted fused derivatives (**161–162**). Antimicrobial screening against Gram-positive and Gram-negative bacteria revealed generally poorly activity, with thione derivative **158a** showing enhanced efficacy against *S. aureus* and *B. subtilis*, while **158d** demonstrated selective inhibition of *B. subtilis* (Table 3).

Table 2 The antibacterial activity of compounds **155b**, **155f**, **156a** and **156b**

Compd	Bacteria	
155b	*S. aureus*	7
155f	*P. aeruginosa*	9
156a	*S. aureus*	7
156b	*P. aeruginosa*	9
Compd	Bacteria	MIC (μg mL^{-1})

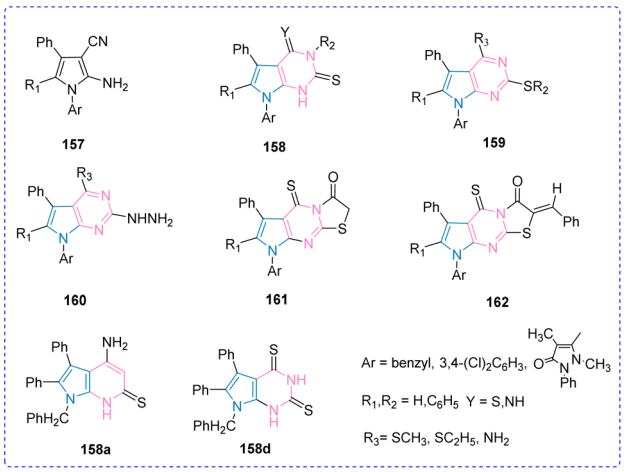

Scheme 31 Structure of compounds **157–162**.

Table 3 The antibacterial activity of compounds **158a** and **158d**

Compd	Anti-*B. subtilis* activity/MIC (μg mL^{-1})
158a	512
158d	512

In the same year, Hassan Hilmy *et al.* (2010) reported synthetic methodologies for novel pyrrolo derivatives and pyrrolo[2,3-*d*]pyrimidine analogues (Scheme 32).[19] Antimicrobial evaluation highlighted significant activity against Gram-positive *S. aureus* for derivatives **164b–d**, **166a–b**, **166e**, **169a**, **d**, and **170c**. Remarkably, compounds **164b–c** and **166e** achieved equivalent efficacy to ampicillin (MIC = 0.62 mg mL^{-1}) against Gram-negative *E. coli*. SAR analysis revealed optimal bioactivity in pyrrolo[2,3-*d*]pyrimidines bearing amino **164a–d**, hydrazino **166a–e**, or diamino **169a–d** substituents, whereas fused triazolo/tetrazolo-pyrimidine systems exhibited reduced potency. Among these compounds, derivatives **164b**, **164c**, and **166e** emerged as the most potent against *S. aureus*, with MIC values of 0.31 mg mL^{-1} – twice the potency of ampicillin (0.62 mg mL^{-1}) (Table 4).

3.1.1 FtsZ inhibtor. The filamenting temperature-sensitive mutant Z (FtsZ) protein, a conserved bacterial cell division component, polymerizes through GTP-dependent mechanisms to form midcell Z-rings. These structures coordinate division machinery assembly, driving septal formation through constriction.[66,67] As a phylogenetically conserved therapeutic target, FtsZ has emerged as a focus for novel bactericide development.[68]

In 2024, Li *et al.* implemented a scaffold-hopping strategy to design 7*H*-pyrrolo[2,3-*d*]pyrimidine derivatives targeting *Xanthomonas oryzae* pv. *oryzae* (*Xoo*) FtsZ (Fig. 3).[69] *In vitro* evaluations identified compound **171** as the most potent agent against *Xoo* (EC_{50} = 4.65 μg mL^{-1}). Mechanistic studies revealed that compound **171** inhibited *Xoo*FtsZ GTPase activity (IC_{50} = 235.0 μM) by potentially interacting with Asn34, Asp38, Val322, and Ala323 on FtsZ, further induced bacterial cell elongation, and thereby causing lethality. SAR analysis showed that alkyl groups enhanced antibacterial activity more effectively than sulfonyl,

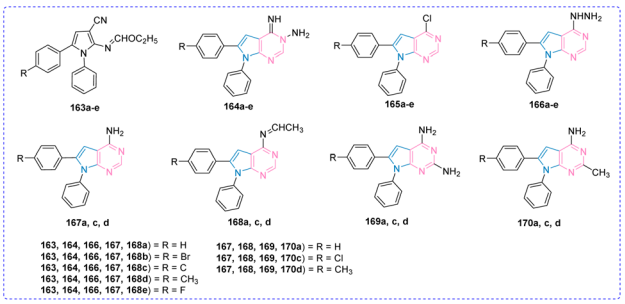

Scheme 32 Structure of compounds **163–166a–e**, **167–170a**, **c**, **d**.

Table 4 The antibacterial activity of compounds **164a**, **164c** and **166e**

	Antibacterial activity/MIC (mg mL^{-1})	
Compd	*S. aureus*	*C. albicans*
164a	0.31	0.62
164c	0.31	0.31
166e	0.31	0.31
Ampicillin	0.62	—

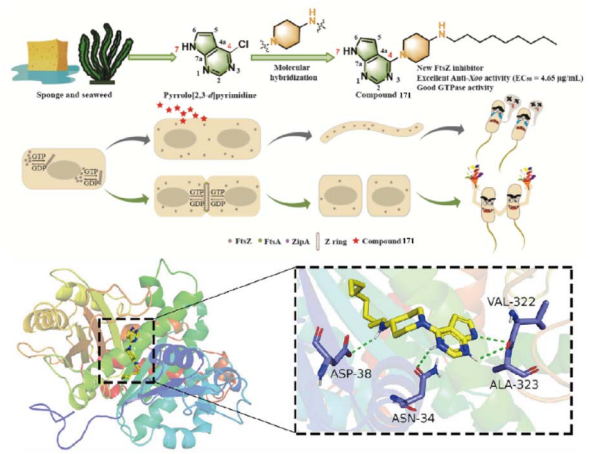

Fig. 3 Synthesis of pyrrolo[2,3-*d*]pyrimidines derivative **171** its bactericidal mechanism. Reproduced from ref. 69 with permission from Elsevier copyright 2024.

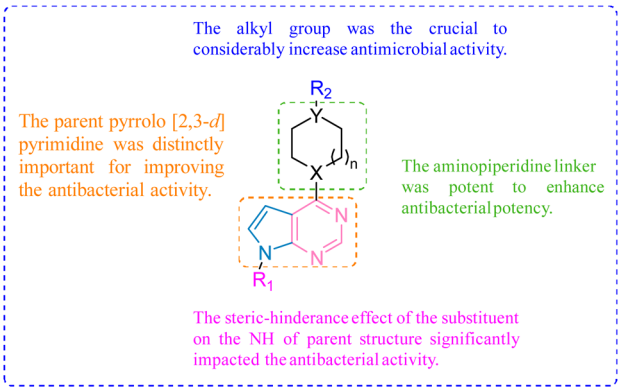

Fig. 4 Structure–activity relationship (SAR) analyses.

acyl, and thiourea groups. The length of the alkyl carbon chain was related to antibacterial activity, showing a trend of first increasing, then stabilizing, and finally decreasing (Fig. 4). Interestingly, this study marks the inaugural application of the pyrrolo[2,3-*d*]pyrimidine scaffold in FtsZ-targeted bactericide development.

3.1.2 DHFR inhibitor. Dihydrofolate reductase (DHFR), an evolutionarily conserved NADPH-dependent oxidoreductase, mediates the stereospecific reduction of dihydrofolate (DHF) to tetrahydrofolate through nicotinamide adenine dinucleotide phosphate (NADPH)-derived hydride transfer, concurrently producing $NADP^+$.[70] Functioning as the principal cofactor in nucleotide biosynthesis and methylation pathways, THF critically sustains fundamental cellular processes including DNA replication and amino acid metabolism.[71] This biochemical essentiality underpins DHFR's status as a prime pharmacological target.[72] Building upon the clinical success of trimethoprim (**TMP**), the first bacterial DHFR inhibitor introduced in the 1960s, Kuyper *et al.* designed conformationally restricted **TMP** analogues through structure-guided optimization (Fig. 5 and Scheme 33).[70] The derivative **175** successfully mimics the **TMP**–

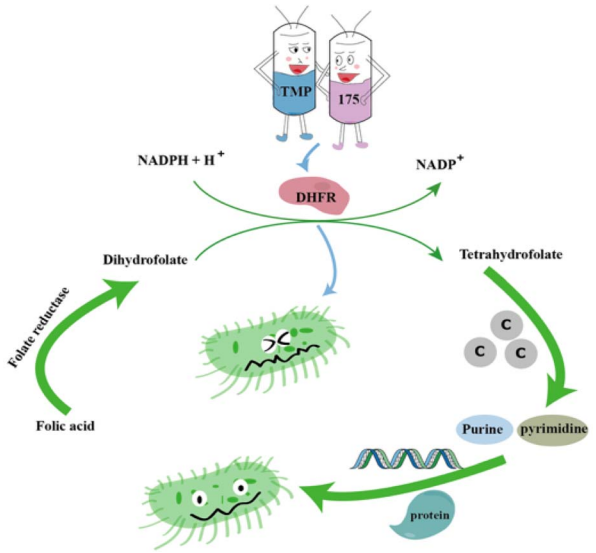

Fig. 5 Hypothetical model depicting the mechanism of action for interference with the bacterial DHFR by compounds **175** and **TMP**.

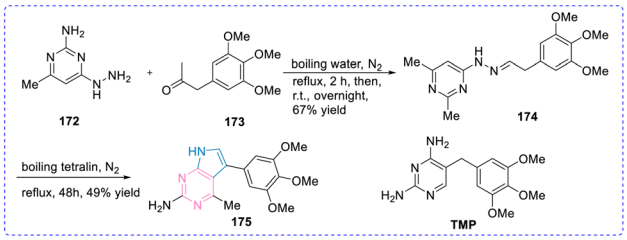

Scheme 33 Synthesis of pyrrolo[2,3-*d*]pyrimidines derivative **175** and the structure of compound **TMP**.

Table 5 DHFR inhibition activity for compound **175** and **TMP**

	IC_{50} (μM)			
Compd	*S. aureus* DHFR	*P. berghei* DHFR	*E. coli* DHFR	*N. gonorrhoeae* DHFR
175	0.039	0.41	0.44	0.18
TMP	0.047	0.24	0.007	0.45

DHFR complex geometry while maintaining comparable bacterial enzyme inhibition. Strikingly, protonated **175** exhibited >10-fold potency enhancement over **TMP** in enzymatic assays, establishing ionization state as a crucial determinant of target affinity (Table 5).

3.1.3 DprE1 inhibitor. In 2019, Shiva Raju's group developed an efficient synthetic route to novel 1-triazolylpyrrolo[2,3-*d*]pyrimidine derivatives *via* intermolecular 1,3-dipolar cyclization, achieving high yields and purity (Scheme 34).[73] Biological evaluation revealed potent antitubercular activity against *M. tuberculosis*, with lead compounds displaying MIC values of 0.78 μg mL^{-1} comparable to reference drugs ciprofloxacin and ethambutol. Additional derivatives exhibited moderate efficacy (MIC range: 3.25–6.25 μg mL^{-1}). Molecular docking analyses

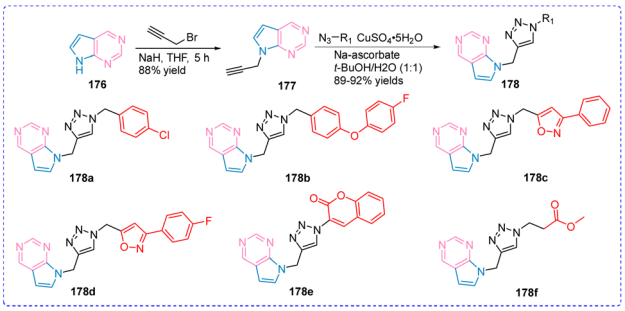

Scheme 34 The structure of compounds **177a–f**.

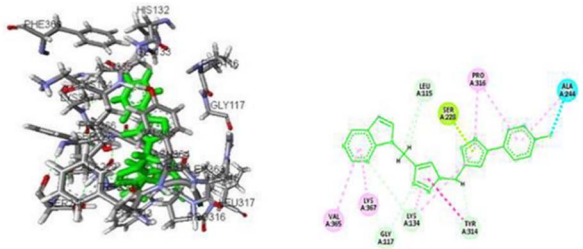

Fig. 6 Molecular docking of **178d** with *M. tuberculosis* DprE1. Reproduced from ref. 73 with permission from Elsevier copyright 2019.

Table 6 The antitubercular activity for compounds **178a–f**

Compd	Antitubercular MIC (μg mL^{-1})
178a	3.12
178b	3.12
178c	0.78
178d	0.78
178e	3.12
178f	1.56

revealed that compound **178d** formed hydrogen bonds with six residues (Val365, Lys367, Lys134, Ser228, Pro316, and Leu115) of the essential cell wall biosynthesis enzyme DprE1, whereas **178c** interacted with Tyr314, His132, and Cys387 alongside sharing common binding residues with **178d** (Fig. 6). The SAR

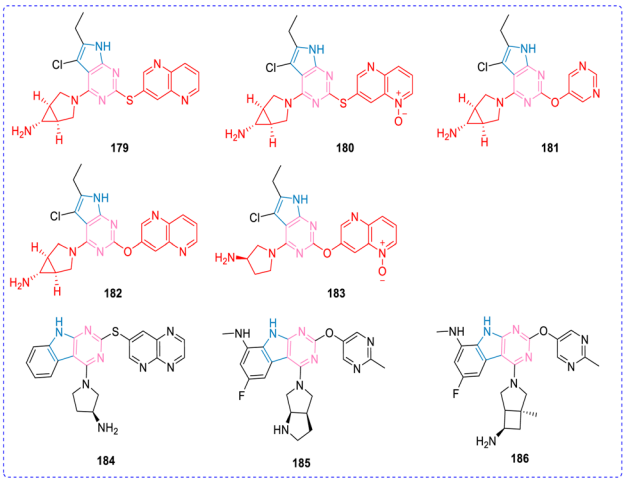

Scheme 35 The structure of compounds **179–186**.

analysis further demonstrated enhanced potency for heteroaryl-substituted triazole derivatives, as evidenced by the superior MolDock and Rerank scores of compounds **178c** and **178d**, which suggests their promising potential as anti-TB agents (Table 6).

3.1.4 GyrB/ParE inhibitor. Bacterial type II topoisomerases DNA gyrase (GYRA/GYRB) and topoisomerase IV (PARC/PARE) represent structurally homologous yet functionally distinct antimicrobial targets.[74,75] These A2B2 holoenzymes regulate DNA topology during replication: DNA gyrase primarily facilitates replication initiation and elongation through negative supercoiling, while topoisomerase IV mediates chromosome decatenation during replication termination.[76] Their essential mechanistic roles and multiple druggable sites make them prime targets for antibacterial development (Table 7).

Tari's team pioneered pyrrolopyrimidine-based inhibitors through pharmacophore-driven discovery in 2013, synthesizing compounds **179–183** (Scheme 35) with optimized Gram-negative penetration and efflux pump resistance circumvention.[60,77] These agents exert bactericidal effects *via* selective topoisomerase inhibition (Fig. 7). Systematic structural optimization by the modifications at R_2, R_4 and R_5 positions, and by comparing the activity of S- and O-linked inhibitors with the same modifications (Table 8), it was demonstrated that

Table 7 The ability of compounds **179–186** to bind GyrB/ParE

	K_i (nM)		K_i (nM)		K_i (nM)	
Compd	*F. tularensis* GyrB	*F. tularensis* ParE	*E. coli* GyrB	*E. coli* ParE	*E. faecalis* GyrB	*E. faecalis* ParE
179	<0.3	0.6	<0.3	1.1	—	—
180	<0.3	2.5	<0.3	1.7	—	—
181	<0.3	1.8	0.4	3.4	—	—
182	<0.3	0.6	<0.3	0.9	—	—
183	<0.3	1.1	<0.3	4.6	—	—
184	520	856	350	536	650	408
185	<0.3	<0.4	<0.05	<0.1	<0.3	<0.3
186	<0.3	0.8	0.3	0.9	<0.3	<0.3

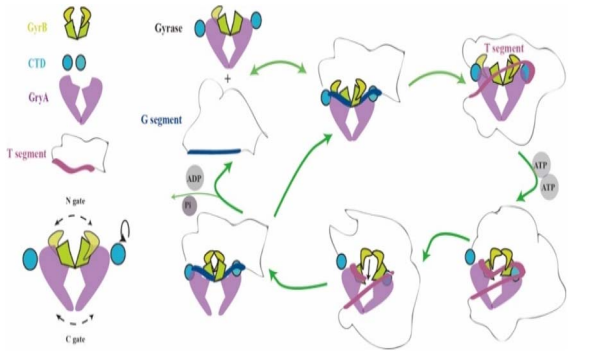

Fig. 7 Gyrase mechanism.

alleviating conformational strain using an O-linker enhances activity, demonstrated that alleviating conformational strain using an O-linker enhances activity. Its unique dual-targeting mechanism exhibited nanomolar potency and single-digit μg mL^{-1} MIC values. Parallel development of tricyclic GyrB/ParE (TriBE) inhibitors yielded pyrrolo[2,3-*d*]pyrimidine derivatives **184–186**.[78] Structural incorporation of a benzene ring in the pyrrole system markedly improved GyrB/ParE affinity compared to bicyclic analogues. Fluorination at the 6-position of benzene (compounds **185–186**) generated broad-spectrum agents with MICs < 0.2 μg mL^{-1} against clinically relevant Gram-positive and Gram-negative pathogens.

Vazirimehr and colleagues (2017) developed two novel pyrrolo[2,3-*d*]pyrimidine derivatives (**189** and **190**) through a multistep synthesis involving: (1) glacial acetic acid-mediated or ultrasonication-assisted reaction of 2-amino-1-methyl-4,5-diphenyl-1*H*-pyrrolo-3-carbonitrile with triethyl orthoformate, followed by sequential condensation with methylamine/benzylamine *via* reflux condition (Scheme 36).[18] The optimized protocol afforded compounds **189** and **190** in 90% and 85% yields respectively. Antimicrobial evaluation revealed modest activities, with both derivatives demonstrating MIC values of 5 and 6 mg mL^{-1} against *S. aureus* and *E. coli*, respectively, while exhibiting slightly improved activity against *M. luteus* (3–4 mg mL^{-1}). These results indicated limited antibacterial efficacy across the tested bacterial strains (Table 9).

3.1.5 ThrRS inhibitor. Aminoacyl-tRNA synthetases (AARS), an evolutionarily conserved enzyme family, execute the essential biochemical task of coupling amino acids with their cognate

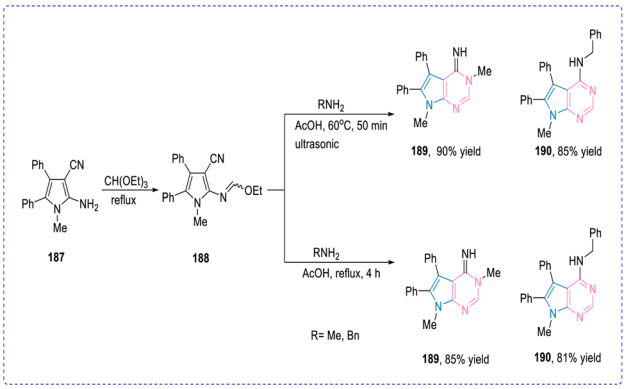

Scheme 36 Synthesis of pyrrolo[2,3-*d*]pyrimidines using catalyst-containing glacial acetic acid or ultrasonic radiation pyrimidine derivatives.

Table 9 The antibacterial activity of compounds **189**, **190**

	Antibacterial activity MIC (mg mL^{-1})		
Compd	*S. aureus*	*E. coli*	*M. luteus*
189	5	6	3
190	5	6	4

tRNAs to maintain translational fidelity. These 20 type-specific catalysts (classified as I/II based on active site architecture)[79,80] include threonyl-tRNA synthetase (ThrRS) a type II enzyme whose inhibition disrupts bacterial protein biosynthesis through misaminoacylation, ultimately causing cell death (Fig. 8). This mechanistic vulnerability establishes ThrRS as an attractive antimicrobial target.

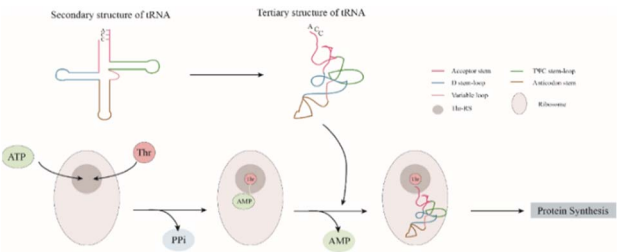

Fig. 8 Involvement of ThrRS in protein synthesis.

Table 8 The antibacterial activity of compounds **179–183**, **185–186**

	Antibacterial activity MIC (μg mL^{-1})						
Compd	*S. aureus*	*S. pneumoniae*	*H. influenzae*	*E. coli*	*K. pneumoniae*	*A. baumannii*	*P. aeruginosa*
179	≤0.06	0.13	4	4	>64	8	8
180	≤0.06	0.25	2	2	32	4	4
181	1	2	4	4	64	16	32
182	≤0.06	≤0.06	1	4	32	4	8
183	0.13	1	4	4	32	8	6
185	0.008	0.001	0.031	0.125	2	0.125	2
186	0.004	0.001	0.031	0.125	1	0.25	1

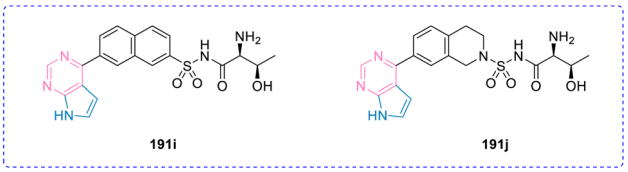

Scheme 37 The structure of 4-substituted pyrrolo[2,3-*d*]pyrimidine derivatives.

In 2013, Teng *et al.* identified a series of ThrRS synthetase inhibitors by using a structure-based drug design (Scheme 37).[81] They are all sulfonamide-substituted nitrogen-containing heterocycles, including quinazolines, isoquinolines, pyrimidines, and pyrrolopyrimidines. These inhibitors bind to the substrate binding site of ThrRS synthetase and show excellent binding affinity for bacterial ThrRS synthetase. Several compounds have improved selectivity for bacterial ThrRS synthetase. Compounds **191i** and **191j** are 4-substituted pyrrolo [2,3-*d*]pyrimidine derivatives, and **191i** binds to *E. coli* with a ThrRS K_i of 2.4 nM more strongly than the other two bacteria (*B. thail* ThrRS K_i = 0.6 nM and *Y. pestis* ThrRS K_i = 1.8 nM). Surprisingly, the ThrRS binding capacity of **191j** was stronger than that of **191i** for the three bacteria mentioned above, *E. coli* ThrRS K_i = 9.5 nM, *B. thail* ThrRS K_i = 4 nM, and *Y. pestis* ThrRS K_i = 5.7 nM, respectively. Notably, **191j** demonstrated >10-fold selectivity for bacterial *versus* human ThrRS, suggesting favorable therapeutic potential. This marked selectivity contrast with **191i** which showed negligible species discrimination highlights critical structural determinants for target specificity while underscoring potential mammalian toxicity concerns with non-selective inhibitors.

3.2 Antifungal activity

In 2002, El-Gaby and colleagues pioneered hybrid antimicrobials through strategic integration of pyrrolo[2,3-*d*]pyrimidine

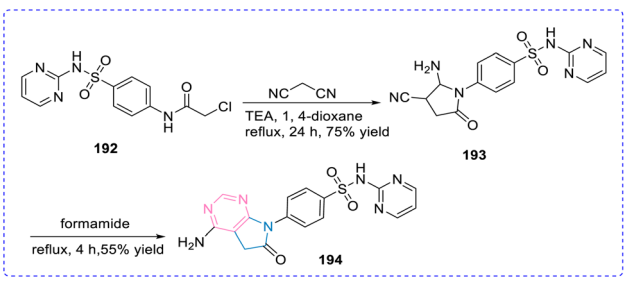

Scheme 38 Synthesis of compound **194**.

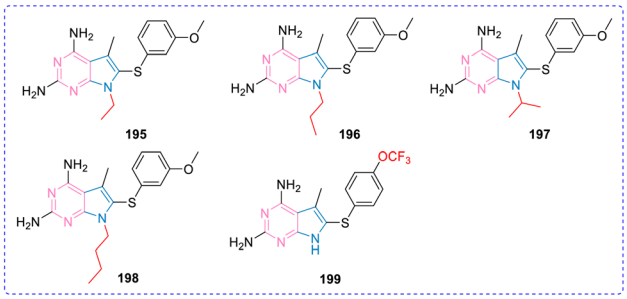

Scheme 39 The structure of compounds **195–199**.

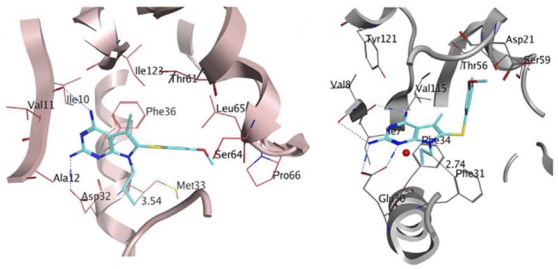

Fig. 9 Docked pose of **195** (cyan) in the homology model of *pj*DHFR (left); docked pose of **190** (cyan) in the crystal structure of hDHFR (right). Reproduced from ref. 82 with permission from Elsevier copyright 2018.

cores with sulfonamide pharmacophores, yielding novel derivatives *via* synthetic route Scheme 38.[82] Structural optimization revealed critical design principles: incorporation of heterocyclic sulfonamide moieties at the pyrrole position enhanced antifungal efficacy, while unsubstituted sulfonamide derivatives showed attenuated or abolished activity. Among synthesized analogs, compound **194** demonstrated broad-spectrum fungicidal activity with approximately 85% efficacy against four pathogenic fungi, though failing to surpass the reference standard mycostatine in potency (Table 10).

In 2018, Shah's team employed structure-guided drug design leveraging human DHFR X-ray crystallographic data and *P. jirovecil* DHFR homology modeling to develop selective anti-pneumocystis agents (Scheme 39).[82] Rational design leveraged critical structural variations at residues Met33 and Phe31, where distinct spatial occupancy between pjDHFR and hDHFR governs inhibitor selectivity (Fig. 9). This approach yielded pyrrolo[2,3-*d*]pyrimidine derivatives **195–199** demonstrating enhanced *pj*DHFR inhibition (IC_{50} values) and significant

Table 10 The inhibition zone diameter method was used to determine the antibacterial activity of compound **194**

	Inhibition zone diameter, mm (relative inhibition)			
Compd	*A. ochraceus* Wilhelm	*P. chrysogenum* Thom	*A. fleavus* Link	*C. albicans* (Robin) Berkho
194	18 (45%)	14 (37%)	16 (42%)	34 (85%)
Mycostatine	40 (100%)	38 (100%)	38 (100%)	40 (100%)

Table 11 Inhibition concentrations against *pj*DHFR and hDHFR and selectivity ratios

	IC_{50} (nM)		
Compd	*pj*DHFR	hDHFR	Selectivity ratio [hDHFR/*pj*DHFR]
195	35	511	15
196	84	2046	24
197	74	579	8
198	73	1130	15
199	81	811	10
TMP	92	24 500	266
PTX	41	2	0.05

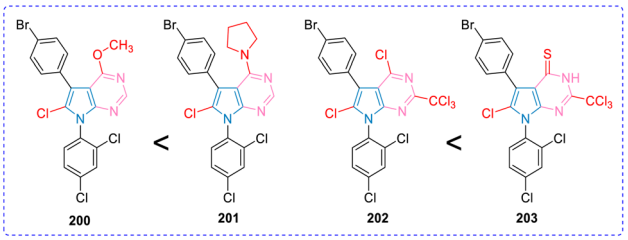

Scheme 40 The structure of compounds **200–203**.

Table 12 The anti-BVDV activity of the synthesized compounds **200–203**

Compd	0.1 mg mL^{-1}
200	90% anti-BVDV
201	100% anti-BVDV
202	90% anti-BVDV
203	100% anti-BVDV

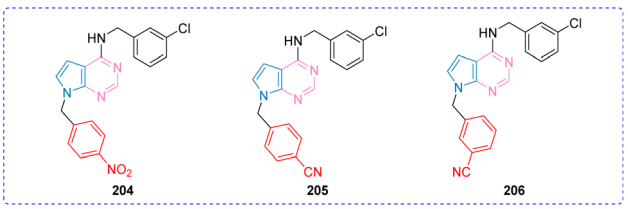

Scheme 41 The structure of compounds **204–206**.

selectivity over human DHFR compared to prototype inhibitor piritrexim. Four compounds exhibited 24-fold *pj*DHFR preference in binding assays (Table 11), with lead compound **196** showing 84 nM potency against *pj*DHFR (24 × selectivity *vs.* hDHFR). SAR results revealed maximal activity with N7-propyl substituents; elongation to *n*-butyl or branching with isopropyl groups failed to improve potency or selectivity, thereby establishing propyl as the optimal N7 chain length for this series.

3.3 Antiviral activity

In 2019, Sroor's team developed structurally diversified pyrrolo[2,3-*d*]pyrimidine derivatives through rational molecular design, subsequently evaluating their antiviral potential against bovine viral diarrhea virus (BVDV).[83] Initial screening identified compounds **200**, **201**, **202**, and **203** as superior inhibitors through direct viral replication assays. SAR studies established critical substitution patterns: optimal anti-BVDV activity occurred when position C2 contained either hydrogen atoms or trichloromethyl groups, coupled with C4 substitutions by chlorine, sulfur, pyrrolidine, or methoxy moieties. This specific substitution pattern demonstrated enhanced viral inhibition compared to analogs bearing chlorine atoms or methyl groups at C2 (Scheme 40).

In 2021, Soto-Acosta and colleagues identified compound **204** as a potent Zika virus (ZIKV) inhibitor, demonstrating EC_{50} = 5.25 μM (reporter assay) and CC_{50} = 20.0 μM, yielding a selectivity index (SI) of 3.81 (Table 12).[84] Building on this lead, systematic structural optimization of the 7*H*-pyrrolo[2,3-*d*]pyrimidine scaffold at positions 4 and 7 yielded analogs **204–206** (Scheme 41), which exhibited enhanced anti-ZIKV potency. The SAR results showed that introducing a simple electron-withdrawing group, preferably nitro or cyano, at the *para* or *meta* position led to excellent anti-ZIKV activity, especially in terms of titer-reducing capability. Notably, these derivatives demonstrated broad-spectrum activity all three compounds (**204–206**) showed >90% protection against dengue virus (DENV) in cellular infection models. Although the specific molecular targets of action remain to be elucidated, 4,7-disubstituted 7*H*-pyrrolo[2,3-*d*]pyrimidines and their analogs are expected to be a new chemotype for the design of against flaviviruses (Table 13).

Table 13 The anti-ZIKV activity of the compounds **204–206**

	ZIKV reporter assay				Titer reduction assay				
Compd	Inhibition (%) at 10 μM	Viability (%) at 10 μM	EC_{50} (μM)	% at 8.5 μM	% at 1.5 μM	EC_{50} (μM)	EC_{90} (μM)	EC_{99} (μM)	CC_{50} (μM)
204	73	69	5.25	93	—	5.21	10.7	—	20.0
205	78	68	4.10	97	47	4.29	9.02	13.6	20.6
206	90	60	3.16	99	—	5.05	6.98	12.7	5.3

4. Conclusion

Pyrrolo[2,3-*d*]pyrimidines have emerged as a privileged scaffold in medicinal chemistry since their initial discovery in the mid-20th century. These bicyclic heterocycles, characterized by their fused pyrrole and pyrimidine rings, have evolved into versatile platforms for drug discovery through innovative synthetic approaches. This review systematically examines two principal cyclization pathways differentiated by their formation sequence of the central pyrrole and peripheral pyrimidine rings – that underpin the scaffold's structural diversification. Contemporary synthetic strategies including microwave-assisted synthesis, solid-phase combinatorial approaches, tandem one-pot methodologies, and Diels–Alder cyclization have enabled efficient access to structural analogs with remarkable stereochemical control and functional group tolerance.

Pharmacological evaluations reveal broad-spectrum antimicrobial potential, particularly against emerging drug-resistant pathogens. Specific derivatives demonstrate potent activity against methicillin-resistant *S. aureus*, *M. tuberculosis* and, and the opportunistic fungus *P. jirovecil*. Notably, select analogs exhibit dual antiviral efficacy against both the BVDV and ZIKV, suggesting potential for pan-antiviral development. These findings position pyrrolo[2,3-*d*]pyrimidines as a strategic chemotype for addressing the global antimicrobial resistance crisis.

The continued advancement of pyrrolo[2,3-*d*]pyrimidine research is poised to focus on several pivotal directions. First, rational design strategies employing computational chemistry, such as QSAR modeling and molecular docking, will guide the optimization of ADMET (absorption, distribution, metabolism, excretion, and toxicity) profiles while enhancing target selectivity and minimizing off-target effects.[85–87] Concurrently, systematic studies on resistance mechanisms using genomic and proteomic approaches will elucidate structure–resistance relationships, informing the design of next-generation analogs capable of circumventing pathogen defenses. Leveraging the scaffold's inherent pharmacophoric versatility, efforts in polypharmacology could yield dual- or multi-target inhibitors to combat complex diseases through synergistic mechanisms. To address bioavailability challenges, innovative drug delivery platforms, including nanoparticle-encapsulated formulations, may revolutionize therapeutic efficacy by improving tissue targeting and pharmacokinetics.[88,89] Beyond antimicrobial applications, expanded exploration into anti-cancer, anti-inflammatory, and neurodegenerative disease models *via* high-throughput phenotypic screening could unlock novel therapeutic niches. Additionally, the integration of green chemistry principles, such as continuous flow synthesis and biocatalytic methods, will promote sustainable large-scale production. These multifaceted endeavors demand interdisciplinary collaboration across medicinal chemistry, pharmacology, and materials science to transform pyrrolo[2,3-*d*]pyrimidine derivatives into clinically actionable therapies for emerging global health threats.

Author contributions

Sun Zhaoju: writing – original draft and visualization. Li Ting: writing – original draft and visualization. Yi He: writing – original draft and visualization. Hongwu Liu: investigation. Linli Yang: investigation. Zhibing Wu: investigation. Liwei Liu: investigation. Zhenbao Luo: funding acquisition, project administration. Xiang Zhou: investigation, funding acquisition, writing – review & editing. Song Yang: supervision, funding acquisition, project administration, writing – review & editing. All authors have read and agreed to the published version of the manuscript.

Conflicts of interest

There are no conflicts to declare.

Data availability

No primary research results, software or code have been included and no new data were generated or analysed as part of this review.

Acknowledgements

This research was financially supported by National Natural Science Foundation of China (32372610, U23A20201, 32160661, 32202359), National Key Research and Development Program of China (2022YFD1700300), the Central Government Guides Local Science and Technology Development Fund Projects [Qiankehezhongyindi (2023) 001] and [Qiankehezhongyindi (2024) 007], and Bijie Tobacco Project (No. 2024SMXM02).

References

1 A. J. Alanis, *Arch. Med. Res.*, 2005, **36**, 697–705.
2 C. Bailly, P. Colson and C. Houssier, *Biochem. Biophys. Res. Commun.*, 1998, **243**, 844–848.
3 T. A. Davies, L. M. Kelly, D. B. Hoellman, L. M. Ednie, C. L. Clark, S. Bajaksouzian, M. R. Jacobs and P. C. Appelbaum, *Antimicrob. Agents Chemother.*, 2000, **44**, 633–639.
4 M. Yenjerla, C. Cox, L. Wilson and M. A. Jordan, *J. Pharmacol. Exp. Ther.*, 2009, **328**, 390–398.
5 P. Nauš, R. Pohl, I. Votruba, P. Džubák, M. Hajdúch, R. Ameral, G. Birkuš, T. Wang, A. S. Ray, R. Mackman, T. Cihlar and M. Hocek, *J. Med. Chem.*, 2010, **53**, 460–470.
6 L. M. De Coen, T. S. A. Heugebaert, D. García and C. V. Stevens, *Chem. Rev.*, 2016, **116**, 80–139.
7 A. E. Rashad, T. El Malah and A. H. Shamroukh, *Curr. Org. Chem.*, 2024, **28**, 1244–1264.
8 M. Y. Chu, L. B. Zuckerman, S. Sato, G. W. Grabtree, A. E. Bogden, M.-I. Lim and R. S. Klein, *Biochem. Pharmacol.*, 1984, **33**, 1229–1234.
9 M. I. Lim, R. S. Klein and J. J. Fox, *J. Org. Chem.*, 1979, **44**, 3826–3829.
10 K. V. B. Rao, W. Y. Ren, J. H. Burchenal and R. S. Klein, *Nucleosides Nucleotides*, 1986, **5**, 539–569.
11 M. I. Lim, W. Y. Ren, B. A. Otter and R. S. Klein, *J. Org. Chem.*, 1983, **48**, 780–788.
12 M. I. Lim and R. S. Klein, *Tetrahedron Lett.*, 1981, **22**, 25–28.

13 R. Wu, E. D. Smidansky, H. S. Oh, R. Takhampunya, R. Padmanabhan, C. E. Cameron and B. R. Peterson, *J. Med. Chem.*, 2010, **53**, 7958–7966.
14 B. Yu, X. P. Shentu and X. P. Yu, *Chin. J. Biol. Control*, 2011, **27**, 373–377.
15 X. P. Shentu, B. Yu, Y. L. Bian, L. Hu, Z. Ma, Z. Y. Tong and X. P. Yu, *Acta Pharm. Sin. B*, 2012, **42**, 105–109.
16 R. M. Hekman, A. J. Hume, R. K. Goel, K. M. Abo, J. Huang, B. C. Blum, R. B. Werder, E. L. Suder, I. Paul, S. Phanse, A. Youssef, K. D. Alysandratos, D. Padhorny, S. Ojha, A. Mora-Martin, D. Kretov, P. E. A. Ash, M. Verma, J. Zhao, J. J. Patten, C. Villacorta-Martin, D. Bolzan, C. Perea-Resa, E. Bullitt, A. Hinds, A. Tilston-Lunel, X. Varelas, S. Farhangmehr, U. Braunschweig, J. H. Kwan, M. McComb, A. Basu, M. Saeed, V. Perissi, E. J. Burks, M. D. Layne, J. H. Connor, R. Davey, J.-X. Cheng, B. L. Wolozin, B. J. Blencowe, S. Wuchty, S. M. Lyons, D. Kozakov, D. Cifuentes, M. Blower, D. N. Kotton, A. A. Wilson, E. Mühlberger and A. Emili, *Mol. Cell*, 2020, **80**, 1104–1122.
17 R. Kazlauskas, P. T. Murphy, R. J. Wells, J. A. Baird-Lambert and D. D. Jamieson, *Aust. J. Chem.*, 1983, **36**, 165–170.
18 S. Vazirimehr, A. Davoodnia, S. A. Beyramabadi, M. Nakhaei-Moghaddam and N. Tavakoli-Hoseini, *Z. Naturforsch., B: J. Chem. Sci.*, 2017, **72**, 481–487.
19 K. M. H. Hilmy, M. M. A. Khalifa, M. A. A. Hawata, R. M. A. Keshk and A. A. El-Torgman, *Eur. J. Med. Chem.*, 2010, **45**, 5243–5250.
20 M. S. Mohamed, A. I. Sayed, M. A. Khedr and S. H. Soror, *Bioorg. Med. Chem.*, 2016, **24**, 2146–2157.
21 M. S. Mohamed, A. I. Sayed, M. A. Khedr, S. Nofal and S. H. Soror, *Eur. J. Pharm. Sci.*, 2019, **127**, 102–114.
22 M. S. Mohamed, A. E. Rashad, M. Adbel-Monem and S. S. Fatahala, *Z. Naturforsch., C: J. Biosci.*, 2007, **62**, 27–31.
23 C. Keenan, K. E. Nichols and S. Albeituni, *Front. Immunol.*, 2021, **12**, 614704.
24 M. Onda, K. Ghoreschi, S. Steward-Tharp, C. Thomas, J. J. O'Shea, I. H. Pastan and D. J. FitzGerald, *J. Immunol.*, 2014, **193**, 48–55.
25 P. Perlíková and M. Hocek, *Med. Res. Rev.*, 2017, **37**, 1429–1460.
26 L. Sun, J. Cui, C. Liang, Y. Zhou, A. Nematalla, X. Wang, H. Chen, C. Tang and J. Wei, *Bioorg. Med. Chem. Lett.*, 2002, **12**, 2153–2157.
27 W. Wu, J. Ma, N. Shao, Y. Shi, R. Liu, W. Li, Y. Lin and S. Wang, *PLoS One*, 2017, **12**, e0169229.
28 T. A. Yap, M. I. Walton, L.-J. K. Hunter, M. Valenti, A. De Haven Brandon, P. D. Eve, R. Ruddle, S. P. Heaton, A. Henley, L. Pickard, G. Vijayaraghavan, J. J. Caldwell, N. T. Thompson, W. Aherne, F. I. Raynaud, S. A. Eccles, P. Workman, I. Collins and M. D. Garrett, *Mol. Cancer Ther.*, 2011, **10**, 360–371.
29 S. Q. Hu, Z. C. Zhao and H. Yan, *Bioorg. Chem.*, 2019, **92**, 103232.
30 T. W. Miller, N. A. Traphagen, J. Li, L. D. Lewis, B. Lopes, A. Asthagiri, J. Loomba, J. De Jong, D. Schiff, S. H. Patel, B. W. Purow and C. E. Fadul, *J. Neurooncol.*, 2019, **144**, 563–572.
31 C. J. N. Mathison, Y. Yang, J. Nelson, Z. Huang, J. Jiang, D. Chianelli, P. V. Rucker, J. Roland, Y. F. Xie, R. Epple, B. Bursulaya, C. Lee, M.-Y. Gao, J. Shaffer, S. Briones, Y. Sarkisova, A. Galkin, L. Li, N. Li, C. Li, S. Hua, S. Kasibhatla, J. Kinyamu-Akunda, R. Kikkawa, V. Molteni and J. E. Tellew, *ACS Med. Chem. Lett.*, 2021, **12**, 1912–1919.
32 M. S. Madhurya, V. Thakur, S. Dastari and N. Shankaraiah, *Bioorg. Chem.*, 2024, **153**, 107867.
33 T. Liang, Y. Yang, J. Wang, Z. Xie and X. Chen, *Mini-Rev. Med. Chem.*, 2023, **23**, 1118–1136.
34 F. Musumeci, M. Sanna, G. Grossi, C. Brullo, A. L. Fallacara and S. Schenone, *Curr. Med. Chem.*, 2017, **24**, 2059–2085.
35 A. Davoodnia, M. Bakavoli, R. Moloudi, M. Khashi and N. Tavakoli-Hoseini, *Chin. Chem. Lett.*, 2010, **21**, 1–4.
36 L. V. Frolova, I. V. Magedov, A. E. Romero, M. Karki, I. Otero, K. Hayden, N. M. Evdokimov, L. M. Y. Banuls, S. K. Rastogi, W. R. Smith, S.-L. Lu, R. Kiss, C. B. Shuster, E. Hamel, T. Betancourt, S. Rogelj and A. Kornienko, *J. Med. Chem.*, 2013, **56**, 6886–6900.
37 C. G. Dave and R. D. Shah, *J. Heterocycl. Chem.*, 1998, **35**, 1295.
38 C. G. Dave and N. D. Desai, *J. Heterocycl. Chem.*, 1999, **36**, 729.
39 S. Hess, C. E. Müller, W. Frobenius, U. Reith, K.-N. Klotz and K. Eger, *J. Med. Chem.*, 2000, **43**, 4636–4646.
40 C. Xiao, C. Sun, W. Han, F. Pan, Z. Dan, Y. Li, Z.-G. Song and Y.-H. Jin, *Bioorg. Med. Chem.*, 2011, **19**, 7100–7110.
41 E. C. Taylor and B. Liu, *J. Org. Chem.*, 2001, **66**, 3726–3738.
42 V. Pittalà, G. Romeo, L. Salerno, M. A. Siracusa, M. Modica, L. Materia, I. Mereghetti, A. Cagnotto, T. Mennini, G. Marucci, P. Angeli and F. Russo, *Bioorg. Med. Chem. Lett.*, 2006, **16**, 150–153.
43 S. J. Kaspersen, C. Sørum, V. Willassen, E. Fuglseth, E. Kjøbli, G. Bjørkøy, E. Sundby and B. H. Hoff, *Eur. J. Med. Chem.*, 2011, **46**, 6002–6014.
44 P. Mizar and B. Myrboh, *Tetrahedron Lett.*, 2008, **49**, 5283–5285.
45 H.-S. Choi, Z. C. Zheng, W. Richmond, X. He, K. Y. Yang, T. Jiang, T. Sim, D. Karanewsky, X. J. Gu, V. Zhou, Y. Liu, O. Ohmori, J. Caldwell, N. Gray and Y. He, *Bioorg. Med. Chem. Lett.*, 2006, **16**, 2173–2176.
46 S. Nagashima, T. Hondo, H. Nagata, T. Ogiyama, J. Maeda, H. Hoshii, T. Kontani, S. Kuromitsu, K. Ohga, M. Orita, K. Ohno, A. Moritomo, K. Shiozuka, M. Furutani, M. Takeuchi, M. Ohta and S. Tsukamoto, *Bioorg. Med. Chem.*, 2009, **17**, 6926–6936.
47 L. El Kaïm, L. Grimaud and S. Wagschal, *Org. Biomol. Chem.*, 2013, **11**, 6883.
48 A. L. Rodriguez, C. Koradin, W. Dohle and P. Knochel, *Angew. Chem., Int. Ed.*, 2000, **39**, 2488–2490.
49 K. Aso, K. Kobayashi, M. Mochizuki, N. Kanzaki, Y. Sako and T. Yano, *Bioorg. Med. Chem. Lett.*, 2011, **21**, 2365–2371.
50 S. Paul and A. R. Das, *Catal. Sci. Technol.*, 2012, **2**, 1130.
51 L. Saikia, P. Roudragouda and A. J. Thakur, *Bioorg. Med. Chem. Lett.*, 2016, **26**, 992–998.

52 H. Tan, Y. Liu, C. Gong, J. Zhang, J. Huang and Q. Zhang, *Eur. J. Med. Chem.*, 2021, **223**, 113670.
53 L. Wang, S. K. Desmoulin, C. Cherian, L. Polin, K. White, J. Kushner, A. Fulterer, M.-H. Chang, S. Mitchell-Ryan, M. Stout, M. F. Romero, Z. Hou, L. H. Matherly and A. Gangjee, *J. Med. Chem.*, 2011, **54**, 7150–7164.
54 J. Shi, R. Van De Water, K. Hong, R. B. Lamer, K. W. Weichert, C. M. Sandoval, S. R. Kasibhatla, M. F. Boehm, J. Chao, K. Lundgren, N. Timple, R. Lough, G. Ibanez, C. Boykin, F. J. Burrows, M. R. Kehry, T. J. Yun, E. K. Harning, C. Ambrose, J. Thompson, S. A. Bixler, A. Dunah, P. Snodgrass-Belt, J. Arndt, I. J. Enyedy, P. Li, V. S. Hong, A. McKenzie and M. A. Biamonte, *J. Med. Chem.*, 2012, **55**, 7786–7795.
55 J. Quiroga, P. A. Acosta, S. Cruz, R. Abonía, B. Insuasty, M. Nogueras and J. Cobo, *Tetrahedron Lett.*, 2010, **51**, 5443–5447.
56 A. I. Khalaf, J. K. Huggan, C. J. Suckling, C. L. Gibson, K. Stewart, F. Giordani, M. P. Barrett, P. E. Wong, K. L. Barrack and W. N. Hunter, *J. Med. Chem.*, 2014, **57**, 6479–6494.
57 Q. Dang and J. E. Gomez-Galeno, *J. Org. Chem.*, 2002, **67**, 8703–8705.
58 Z. Janeba, J. Balzarini, G. Andrei, R. Snoeck, E. De Clercq and M. J. Robins, *J. Med. Chem.*, 2005, **48**, 4690–4696.
59 N. G. M. Davies, H. Browne, B. Davis, M. J. Drysdale, N. Foloppe, S. Geoffrey, B. Gibbons, T. Hart, R. Hubbard, M. R. Jensen, H. Mansell, A. Massey, N. Matassova, J. D. Moore, J. Murray, R. Pratt, S. Ray, A. Robertson, S. D. Roughley, J. Schoepfer, K. Scriven, H. Simmonite, S. Stokes, A. Surgenor, P. Webb, M. Wood, L. Wright and P. Brough, *Bioorg. Med. Chem.*, 2012, **20**, 6770–6789.
60 L. W. Tari, M. Trzoss, D. C. Bensen, X. M. Li, Z. Y. Chen, T. Lam, J. Zhang, C. J. Creighton, M. L. Cunningham, B. Kwan, M. Stidham, K. J. Shaw, F. C. Lightstone, S. E. Wong, T. B. Nguyen, J. Nix and J. Finn, *Bioorg. Med. Chem. Lett.*, 2013, **23**, 1529–1536.
61 J. H. Lee and H.-S. Lim, *Org. Biomol. Chem.*, 2012, **10**, 4229.
62 Y. E. Ryzhkova, A. N. Fakhrutdinov and M. N. Elinson, *Tetrahedron Lett.*, 2021, **81**, 153336.
63 C. G. Dave and R. D. Shah, *Molecules*, 2002, **7**, 554–565.
64 R. Ghahremanzadeh, S. C. Azimi, N. Gholami and A. Bazgir, *Chem. Pharm. Bull.*, 2008, **56**, 1617–1620.
65 M. S. Mohamed, R. Kamel and S. S. Fatahala, *Eur. J. Med. Chem.*, 2010, **45**, 2994–3004.
66 E. Bi and J. Lutkenhaus, *Nature*, 1991, **354**, 161–164.
67 J. Errington, R. A. Daniel and D.-J. Scheffers, *Microbiol. Mol. Biol. Rev.*, 2003, **67**, 52–65.
68 K. A. Hurley, T. M. A. Santos, G. M. Nepomuceno, V. Huynh, J. T. Shaw and D. B. Weibel, *J. Med. Chem.*, 2016, **59**, 6975–6998.
69 T. Li, Y. Zhou, X. C. Fu, L. Yang, H. W. Liu, X. Zhou, L. W. Liu, Z. B. Wu and S. Yang, *Bioorg. Chem.*, 2024, **150**, 107534.
70 L. F. Kuyper, J. M. Garvey, D. P. Baccanari, J. N. Champness, D. K. Stammers and C. R. Beddell, *Bioorg. Med. Chem.*, 1996, **4**, 593–602.
71 M. Watson, J. Liu and D. Ollis, *FEBS J.*, 2007, **274**, 2661–2671.
72 R. L. Then, *J. Chemother.*, 2004, **16**, 3–12.
73 K. S. Raju, S. AnkiReddy, G. Sabitha, V. S. Krishna, D. Sriram, K. B. Reddy and S. R. Sagurthi, *Bioorg. Med. Chem. Lett.*, 2019, **29**, 284–290.
74 Z. Xie, B. Oscar, L. Zhao, X. Ding, C. Cao, S. Feng, H. Li, C. Pan, Z. Bian, Y. Li, W. Wang, Y. Kong and Z. Li, *Eur. J. Med. Chem.*, 2017, **125**, 197–209.
75 M. Oblak, M. Kotnik and T. Solmajer, *Curr. Med. Chem.*, 2007, **14**, 2033–2047.
76 C. Sissi and M. Palumbo, *Cell. Mol. Life Sci.*, 2010, **67**, 2001–2024.
77 M. Trzoss, D. C. Bensen, X. Li, Z. Chen, T. Lam, J. Zhang, C. J. Creighton, M. L. Cunningham, B. Kwan, M. Stidham, K. Nelson, V. Brown-Driver, A. Castellano, K. J. Shaw, F. C. Lightstone, S. E. Wong, T. B. Nguyen, J. Finn and L. W. Tari, *Bioorg. Med. Chem. Lett.*, 2013, **23**, 1537–1543.
78 L. W. Tari, X. Li, M. Trzoss, D. C. Bensen, Z. Chen, T. Lam, J. Zhang, S. J. Lee, G. Hough, D. Phillipson, S. Akers-Rodriguez, M. L. Cunningham, B. P. Kwan, K. J. Nelson, A. Castellano, J. B. Locke, V. Brown-Driver, T. M. Murphy, V. S. Ong, C. M. Pillar, D. L. Shinabarger, J. Nix, F. C. Lightstone, S. E. Wong, T. B. Nguyen, K. J. Shaw and J. Finn, *PLoS One*, 2013, **8**, e84409.
79 G. Eriani, M. Delarue, O. Poch, J. Gangloff and D. Moras, *Nature*, 1990, **347**, 203–206.
80 Y. L. J. Pang, K. Poruri and S. A. Martinis, *Wiley Interdiscip. Rev.: RNA*, 2014, **5**, 461–480.
81 M. Teng, M. T. Hilgers, M. L. Cunningham, A. Borchardt, J. B. Locke, S. Abraham, G. Haley, B. P. Kwan, C. Hall, G. W. Hough, K. J. Shaw and J. Finn, *J. Med. Chem.*, 2013, **56**, 1748–1760.
82 M. S. A. El-Gaby, A. M. Gaber, A. A. Atalla and K. A. A. Al-Wahab, *Il Farmaco*, 2002, **57**, 613–617.
83 F. M. Sroor, W. M. Basyouni, W. M. Tohamy, T. H. Abdelhafez and M. K. El-awady, *Tetrahedron*, 2019, **75**, 130749.
84 R. Soto-Acosta, E. Jung, L. Qiu, D. J. Wilson, R. J. Geraghty and L. Chen, *Molecules*, 2021, **26**, 3779.
85 G. Wang, H. Liu, Y. Zhou, L. Zhang, J. Zhang, L. Shao, X. Zhou, Z. Wu, L. Liu and S. Yang, *Pest Manage. Sci.*, 2025, **81**, 5413–5427.
86 H. Liang, Y. M. Feng, D. Zeng, J. R. Zhang, L. Cheng, X. C. Fu, Z. Q Long, X. Zhou, L. W. Liu, Z. B. Wu and S. Yang, *Pest Manage. Sci.*, 2025, **81**, 4348–4364.
87 S. S Su, H. W. Liu, J. R. Zhang, P. Y. Qi, Y. Ding, L. Zhang, L. L. Yang, L. L. Wei, X. Xiang and S. Yang, *J. Integr. Agric.*, 2024, **23**, 1259–1273.
88 P. Y. Qi, L. H. Shi, Z. C. Zheng, Y. M. Feng, T.-H. Zhang, R. S. Luo, S. Tan, A. L. Tang, H. Y. Huang, X. Zhou, H. M. Xiang, L. W. Liu and S. Yang, *Carbohydr. Polym.*, 2025, **363**, 123733.
89 W. B. Shao, R. S. Luo, Y. W. Huang, L. Cheng, D. Zeng, X. Zhou, L.-W. Liu and S. Yang, *Chem. Eng. J.*, 2025, **509**, 161352.